5 Prisoner's Dilemma: a code of conduct application

We have now completed the first part of the book in which we have provided an in-depth development of ***decision process theory***. In this next part of the book, we inquire into the nature of this theory. We focus on the stationary wave aspects as well as delve deeper into the connection of the theory to earlier game theory descriptions. In this chapter we start with the prisoner's dilemma with a single active strategy and three additional codes of conduct. In the next chapter, we consider an even simpler game with a single active strategy and no codes of conduct, the Robinson Crusoe scenario, and discuss a taxonomy or organization for the theory. In chapter 7 we set the context of these examples with a general review of game theory and recent economic approaches.

Before starting this chapter, recall that in section 1.4, we introduced the prisoner's dilemma and noted its connection to *game theory*. The theory developed in the intervening chapters substantially diverges from its game theoretic origins. It is our goal here to show this by quantitatively analyzing the choices prisoners face using the *player fixed frame model*. This application highlights how far we have come theoretically from our starting point and demonstrates how the approach from the last chapter can be applied to give new insights.

For example, we argue that the *player fixed frame model* applied to the prisoner's dilemma demonstrates the stability of solutions that rest on an adopted ***code of conduct*** (section 7.2) of the players, which we believe is an important departure from *game theory*. In this sense the prisoner's dilemma is our "hydrogen atom" for *decision process theory* since it provides an important and solvable model, just as the "hydrogen atom" provides an important and solvable theory for classical and quantum mechanics in physics. The prisoner's dilemma is an example of a contract (exercise 5), which forms the basis of the invisible hand (Smith, 1776).

The prisoner's dilemma has been extensively investigated by game theorists since the late 1950s. The common sense solution to the prisoner's dilemma is to argue that the situation is an example of the tragedy of the commons (section 7.2). The tragedy occurs when both prisoners take from the commons, causing both to suffer. However, this tragedy of the commons is avoided if the prisoners adhere to a common *code of conduct*, which in this case would be to remain silent when questioned. We demonstrate that *codes of conduct* are natural attributes of *decision process theory*. They come into being whenever we identify strategies as *inactive*.

The solutions that result from the field equations can be proved to have a ***mathematical stability*** because small changes to the initial conditions, whether or not the initial symmetry conditions are maintained, lead to small changes in the behaviors of the solutions. The result is a consequence of the differential geometry for Einstein type hyperbolic partial differential equations (Hawking & Ellis, 1973, p. 254).

We observe that ***structural stability*** is also important and distinct from *mathematical stability*. Whether a bridge stands or falls, the laws of physics provide a mathematical stable description; but for it to stand we require the bridge to be *structurally stable*. Since the *player fixed frame model* with the *quasi-stationary hypothesis* has some similarities to a bridge in that there are significant stationary aspects to both, we will also have occasion in our discussion to speculate on whether or not our solutions are also *structurally stable*. As with bridges we look for the tell-tale creaks and groans from the stresses and strains to imagine what might happen if our mathematical assumptions about the stresses were to break down.

The chapter is organized as follows: we start with a discussion of the relevance of altruism and egotism (section 5.1), followed by analyzing the prisoner's dilemma into normal form (section 5.2). We then provide an equivalent formulation of the initial conditions (section 5.3) and introduce the code of

conduct distinction into the theory (section 5.4). We turn then to solutions based on known behaviors (section 5.5), which describe the initial conditions. A key insight from the past chapters is that the theory has stresses (section 5.6) and strains (section 5.7), which are addressed next, followed by a discussion of the other major characteristic of the theory, its persistent behaviors (section 5.8). We then discuss dynamic behaviors (section 5.9) and end with a sensitivity analysis (section 5.10) and a summary of normal-form behaviors (section 5.11).

5.1 *Egoists and altruists*

The results in this section extend previous work, (Thomas & Kane, 2008) and (Thomas & Kane, 2010), which applied a single strategy *player fixed frame model* to the prisoner's dilemma. They modified the forms for the payoffs introduced below in Eq. (5.3) and (5.4), to this model. We shall see that reducing the number of strategies in this way to a single active strategy is equivalent to choosing a *code of conduct* (section 7.2). In this case, public-interest supplements self-interest.

These authors found similarities to the ***decision process theory*** with the ***incomplete games*** proposed by (Harsanyi, 1967-1968), in his trilogy on game theory. The *decision process theory* here goes one step further than Harsanyi in proposing that actions are characterized not only by payoffs, but by ***inertia*** and ***charge***. As with physical systems, *inertia* implies that there must be enough *force* to overcome inertia in changing a system from a given course. Ordinary payoff forces—i.e., the forces that arise from one's beliefs and past experiences—may not be sufficient. The second is the property of *charge*. In their model of public goods games, (Eshel, Samuelson, & Shaked, 1998) described players (subjects) as either *egoists* (who maximize self-interest) or *altruists* (who maximize other-interest). In contrast, (Thomas & Kane, 2010) suggested that Eshel *et al.*'s egoist/altruist distinction corresponds roughly to a well-known and empirically-tested distinction made in psychology regarding *independent* and *interdependent* ***worldviews.*** They refer the reader to (Markus & Kitayama, 1991) for an extensive review. The suggestion is that subjects who possess *independent* worldviews correspond roughly to Eshel *et al.*'s *egoists*, while subjects with *interdependent* worldviews correspond roughly to *altruists*. Based upon this insight, the suggestion was to incorporate the *independent/interdependent* distinction and liken it to the physical property of ***charge***.

We feel that a more satisfactory conclusion (section 7.2) is that the worldview of independence is associated with the players' inactive strategy whereas interdependence is associated with a *code of conduct* that treats as inactive what would otherwise be active strategies. We associate charge (section 7.6) with the ***player's interest flow***, which we characterize as either that of a ***giver*** or ***taker***. This has some of the same sense of the above mentioned authors, though we take the words to be more akin to seller and buyer or producer and consumer. Alternatively we use the terminology ***accommodating*** and ***greedy*** for positive (*giver*) and negative charges (*taker*). We find for the prisoner's dilemma that the more ***aggressive*** player is greedy (*Cf.* section 5.8.4).

Unlike game theoretic approaches, such as (Harsanyi, Games with incomplete information played by "Bayesian" players, I-III, 1967-1968), we do not consider separate *subjective* and *objective* payoff matrices. In *decision process theory*, each player's payoff matrix is a *personal payoff matrix*. That is, each player constructs a payoff matrix that represents what that player believes will result as payoffs to him or her and all other players. These personal payoff matrices are *not* public knowledge within the game: each player constructs and has access only to his or her own personal payoff matrix. However, players learn as the game is played and over time, they come to a more accurate view based on their own outcomes and the outcomes they observe for others. It is reasonable that the payoff matrix will in general change over time.

There are two additional properties of personal payoff matrices that are important. First, although each personal payoff matrix is *private* information rather than *public* information, according to our theory, each personal payoff matrix is *observable* and *measurable*, though it may not be easy to measure. An analogy may be helpful. The field of empirical psychology attempts to understand people's (and occasionally animals') observable behaviors in terms of mental processes that cause them. These mental processes are very difficult to observe, however. The underlying properties of the mental processes are

usually not possible to observe under circumstances that present themselves in the everyday world. In order to understand mental processes, a person's environment needs to be *controlled* in ways that the everyday environment usually does not allow (Stanovich, 2004, p. 92):

> "The occurrence of any event in the world is often correlated with many other factors. In order to separate, to pry apart, the causal influence of many simultaneously occurring events, we must create situations that will never occur in the ordinary world".

When the environment is controlled in this way, mental processes suddenly become observable. This observation about psychology provides insight to the personal payoff matrices. The personal payoff matrices are potentially observable and measurable, but it would be difficult to measure them, especially in the context of a game already in play. This is why players' personal payoff matrices are usually *not* public information within the game. Nonetheless, these personal payoff matrices are still objective and measurable.

The second important property of personal payoff matrices is that each player's personal payoff matrix can be *idiosyncratic*: that is, the players' personal payoff matrices do not have to be identical to each other and most likely depend on what strategies have just been played. If each player generates his or her personal payoff matrix based on his or her past experiences (which are by definition particular to each player), then each player will most likely generate a different personal payoff matrix that depends on strategy and time.

In *decision process theory*, to specify a solution, we provide the initial strategies and initial payoffs for each player; the field equations then provide unique solutions. To compare and contrast our results with *game theory*, we choose as our initial strategies those that game theory might propose as the equilibrium strategies. We choose as our initial payoff matrices those that game theory might propose. If these were to stay the same at all other strategies and all later times, we would recover the game theory Nash equilibrium result. To the extent they change we obtain the deviations of *decision process theory* from *game theory*.

5.2 *Prisoner's dilemma—the story in normal form*

We now put the prisoner's dilemma into *normal form* in this section. We identify the *code of conduct* in section 5.4. From section 1.4 we recall that the essential details of the story are that two prisoners are being held for a crime where it is suspected they have acted in concert. Each is given a choice to confess or not confess with penalties that are supposed to induce confession of their guilt. However if neither confesses they will get off lightly. If both confess they will be penalized but not as severely as the case in which one confesses and implicates the other. We are interested in understanding the decision process that takes place for each of the prisoners. We note that the *game theory* analysis argues that the players will act only based on their self-interest, which leads each of them to conclude that they should confess. The paradox or dilemma is that common sense suggests that there are reasons why both prisoners might choose not to confess, yet this choice is absent in *game theory*. We need to show that both scenarios are possible in *decision process theory* as is also true in real life. The relevant task is to determine the initial conditions and what happens next.

We start with the formulation of the prisoner's dilemma as a game in ***normal form*** between two prisoners specified by the following payoffs to player 1.

G^1_{12}	N_2	C_2
N_1	−0.1	−1
C_1	0	−0.9

(5.1)

There are identical payoffs to player 2:

G^2_{21}	N_1	C_1
N_2	−0.1	−1
C_2	0	−0.9

(5.2)

We suppose that at some initial value of time and at some special strategic point in the strategic space, there are quantitative payoffs for the matrix $\mathbf{G}^k$ of possibilities as illustrated above for each player $k \in \{1,2\}$. We differ from game theory in that these payoffs are not constants for all points of space and time.

At any point in space time, we describe the elements of the matrix in detail for player 1, noting a similar description holds for player 2. For player 1, the rows are labeled (C_1) if player 1 confesses and (N_1) if player 1 does not confess. The columns are labeled in a similar manner (N_2) and (C_2). Our initial choices for the payoffs translate as follows. At the initial point of space and time, the payoffs reflect quantitatively the posed problem: if both confess, player 1 loses $9/10$ units; if both don't confess player 1 loses a much smaller value $1/10$. If player 1 confesses and implicates player 2 who does not confess, then player 1 loses 0 units. On the contrary, if player 1 does not confess and is implicated by player 2, player 1 loses 1 unit. At other values of time and space, the payoff values are computed from the *player fixed frame model*, though we have yet to argue why we make the assumption of a single active strategy.

Though rather simple, the example has several general properties in common with *game theory*. We have payoff matrices and we have mixed strategies. We differ however in our method of computing the mix of strategies from which each player picks. In *game theory*, the mix of strategies is associated with equilibrium.

For example, the payoffs for the two players need not add up to zero; when they do, (Von Neumann & Morgenstern, 1944) such ***zero-sum games*** have an equilibrium value that is computed as follows. Suppose the payoffs Eq. (5.1) for player 1 represented a zero-sum game. The most conservative strategy for player 1 would be to determine the minimum outcome for each of its pure strategy choices. If player 1 chooses (N_1), the minimum case is -1. If player 1 chooses (C_1) the minimum is $-9/10$. The maximum of these two is $-9/10$. The most conservative strategy is to choose this max-min. For pure strategy choices, there may not always be a max-min solution. What (Von Neumann & Morgenstern, 1944) showed however, is that for a zero-sum game with any number of players, each with any number of strategies, there is always a max-min using mixed strategies. This ***equilibrium strategy*** determines the mix of strategies in game theory. For two players for a ***non-zero sum game***, an analogous Nash equilibrium determines the mix of strategies. For the prisoner's dilemma it is that both players choose not to confess. They optimize their self-interest by acting defensively.

To articulate the difference, we don't argue directly with the individual payoffs such as Eq. (5.1) but construct our argument using the *symmetric game* Eq. (1.12):

F^1_{ab}	N_2	C_2	N_1	C_1	t
N_2	0	0	$1/10$	0	0
C_2	0	0	1	$9/10$	$-9/10\zeta^0$
N_1	$-1/10$	-1	0	0	$1/\zeta^0$
C_1	0	$-9/10$	0	0	$9/10\zeta^0$
t	0	$9/10\zeta^0$	$-1/\zeta^0$	$-9/10\zeta^0$	0

(5.3)

We identify the "hedge" strategy with time t and take this payoff to be the value at an initial value of time and at an initial strategic point. We construct the similar payoff for player 2, again evaluated at the same point:

F^2_{ab}	N_2	C_2	N_1	C_1	t
N_2	0	0	$-1/10$	-1	$1/\zeta^0$
C_2	0	0	0	$-9/10$	$9/10\zeta^0$
N_1	$1/10$	0	0	0	0
C_1	1	$9/10$	0	0	$-9/10\zeta^0$
t	$-1/\zeta^0$	$-9/10\zeta^0$	0	$9/10\zeta^0$	0

(5.4)

In *game theory*, it is a property of the Nash equilibrium that the product of the payoff for player 1, Eq. (5.3) and the mixed strategy $\zeta_{Nash} = \{0,1,0,1,\zeta^0\}$ is zero. The similar statement holds for player 2.

Instead, in *decision process theory* we argue that the mix of strategies is determined dynamically. We can pick any mixed strategy for our initial point. Whether or not the initial value changes in time depends on the flow equation that replaces Eq. (1.13). In the *normal-form coordinate basis*, the replacement flow equation is determined by Eq. (1.75) and (3.42):

$$\frac{DV_a}{\partial\tau} = g_{ab}\frac{dV^b}{d\tau} + \varpi_{abc}V^bV^c - V_kF^k_{ab}V^b + \tfrac{1}{2}V_jV_k\partial_a\gamma^{jk} = q_\alpha E_a{}^\alpha \tag{5.5}$$

We see that there are many sources of change besides the payoff term. Conversely, even if that term is non-zero, the other terms can *conspire* to make the flow *stationary*. We thus acknowledge the importance of self-interest, to the extent we apply that loose concept to the forces derived directly from the payoffs. We also must acknowledge the importance of other effects assuming they are not negligibly small. In order to understand the size of such other effects we must appeal to model calculations of the various *conspiracy* effects in Eq. (5.5).

The characteristic of interest for the various effects is the acceleration, which in the *co-moving frame* for the *player fixed frame model*, has only active components q_υ. We see that in the *game theory* approximation, with the initial condition that the acceleration is zero, the acceleration stays zero at all other values of time and space. We break this approximation in the *player fixed frame model*, even when the orientation potentials are static. This is because the variation of the acceleration with distance is determined by the divergence Eq. (4.58):

$$\partial_\upsilon q^\upsilon = \kappa\left(\mu + p - \frac{\mu - p}{n-1}\right) - 2\omega_{\upsilon\alpha}\omega^{\upsilon\alpha} - \omega_{\upsilon\upsilon'}\omega^{\upsilon\upsilon'} + \omega^{\upsilon\alpha}{}_\alpha q_\upsilon + q_\upsilon q^\upsilon \tag{5.6}$$

Whatever the origin of the conspiracy effects, we see no direct evidence here that they are caused by the payoffs. The results are governed by the inertial, charge gradient and tidal effects. This suggests that we may learn a significant amount by considering even the simplest single strategy model in which the payoffs (for the effective players of the model) are greatly simplified. We then focus our study of the effects of Eq. (5.6), further simplifying it since with a single active strategy there are no tidal magnetic effects $\omega_{\upsilon\upsilon} = 0$.

5.3 *Equivalent formulations of the initial conditions*

We now look into various formulations of the prisoner's dilemma that are equivalent to the game theory *normal form*, section 5.2. In *decision process theory*, it is useful to identify these equivalent models, as they may lead to different dynamic consequences. For example, the payoffs for each prisoner could be scaled by arbitrary factors σ_k for each player representing the ***player stakes*** in the decision process. In our *decision process theory*, the dynamic behavior is influenced by these stakes, as we show in our numerical sensitivity analysis.

An important extension to *game theory* is our introduction of the time component ζ^0 of the flow, which leads to the invariant definition of ***decision process mass***:

$$m = \sqrt{\gamma_{\mu\nu}\zeta^\mu\zeta^\nu} \tag{5.7}$$

Nothing in game theory depends on this parameter. If we scale the active and inactive strategies by this mass, we obtain the normalized flow components:

$$V^a = \frac{\zeta^a}{m}$$
$$V^j = \frac{\zeta^j}{m} \tag{5.8}$$

We may be used to thinking of the strategies summing to unity for each player, which highlights the relative strategic values. Now however, we ascribe meaning to the value of each strategy. The features that remain when we scale the strategy to a unit strategy are characterized by the ***beta*** β of the initial values:

$$\beta = \frac{1}{\zeta^0}\sqrt{\sum_a \left(\zeta^a\right)^2 + \sum_j \left(\zeta^j\right)^2} \tag{5.9}$$

The value of beta depends on the active and inactive flow components. For numerical work, if we provide a value for β, we obtain ζ^0 from Eq. (5.9), defined by the initial strategy flow. The decision mass is then obtained from Eq. (5.7).

Another equivalence normally hidden in game theory is the ***game value***, which does not influence the choice of Nash equilibriums. For the prisoner's dilemma, the active strategy space has four dimensions. Since there are two players, the inactive strategy space has two dimensions. The total strategic dimensionality is $n = 6$. The Nash equilibrium for the prisoner's dilemmas is that both players confess: ${\zeta_{Nash}}^b = \{0,1,0,1,m\}$, where m can be chosen arbitrarily at this point. An attribute of game theory is that the *game value* does not dictate the strategic possibilities (choice of Nash equilibrium). Typically, one can add to each game a constant amount leaving these strategic possibilities invariant. In the symmetric form this constant is a matrix:

$$c(v) = \begin{pmatrix} 0 & 0 & -v & -v & v/\zeta^0 \\ 0 & 0 & -v & -v & v/\zeta^0 \\ v & v & 0 & 0 & -v/\zeta^0 \\ v & v & 0 & 0 & -v/\zeta^0 \\ -v/\zeta^0 & -v/\zeta^0 & v/\zeta^0 & v/\zeta^0 & 0 \end{pmatrix} \tag{5.10}$$

We are free to choose any *game value*. Looking at player 1, we see from Eq. (5.3), that no choice makes the time components all zero. We change this for our example.

Our argument is that in our *decision process theory*, the time component of the payoff reflects the bias that we believe accurately reflects the notion of the *game value* from game theory. Not every game need be fair. We have pointed out that we can add an overall constant payoff Eq. (5.10). It should also be possible to frame the prisoner's dilemma in a way that it too could be put into the form of a fair game. The condition is that the time components for each player should be equal and that amount then subtracted from each payoff. We achieve this by adding ***internal payoffs*** to ${F^1}_{ab}$ so that the product ${F^1}_{ab}{\zeta_{Nash}}^b = 0$ of the payoff and the starting strategy ${\zeta_{Nash}}^b$ are zero:

$$\begin{pmatrix} 0 & 9/10 & -4/5 & -9/10 & 0 \\ -9/10 & 0 & 1/10 & 0 & 0 \\ 4/5 & -1/10 & 0 & 1/10 & 0 \\ 9/10 & 0 & -1/10 & 0 & 0 \\ 0 & 0 & 0 & 0 & 0 \end{pmatrix} \begin{pmatrix} 0 \\ 1 \\ 0 \\ 1 \\ \zeta^0 \end{pmatrix} = \begin{pmatrix} 0 \\ 0 \\ 0 \\ 0 \\ 0 \end{pmatrix} \tag{5.11}$$

This payoff plus the constant matrix $c(-9/10)$ from Eq. (5.10) reproduces the same payoffs as the sub matrix Eq. (5.1). There is an internal payoff or utility for player 1 to choose to not confess of $1/10$. For example, without this bias, the return for player 1 for the equilibrium strategy would be negative instead of zero. We thus obtain the same strategic behavior as the symmetrized game Eq. (5.3).

If both players choose to cooperate and not confess (N_1N_2), then player 1 loses $1/10$. If player 1 chooses to cooperate and not confess and player 2 chooses to confess (N_1C_2), then player 1 loses 1 unit. If player 1 chooses to confess and player 2 chooses to cooperate and not confess (C_1N_2), player 1 sees maximum benefit and receives 0. Finally if player 1 and player 2 both choose to confess (C_1C_2), then player 1 loses $9/10$. The Nash equilibrium point is the strategy whose product with the payoff is zero.

In a similar fashion, we choose the payoff for player 2, so that the product ${F^2}_{ab}{\zeta_{Nash}}^b = 0$ is also zero:

$$\begin{pmatrix} 0 & 1/10 & 4/5 & -1/10 & 0 \\ -1/10 & 0 & 9/10 & 0 & 0 \\ -4/5 & -9/10 & 0 & 9/10 & 0 \\ 1/10 & 0 & -9/10 & 0 & 0 \\ 0 & 0 & 0 & 0 & 0 \end{pmatrix} \begin{pmatrix} 0 \\ 1 \\ 0 \\ 1 \\ \zeta^0 \end{pmatrix} = \begin{pmatrix} 0 \\ 0 \\ 0 \\ 0 \\ 0 \end{pmatrix} \tag{5.12}$$

This payoff plus the constant matrix $c(+9/10)$ from Eq. (5.10) reproduces the same payoffs as the sub matrix Eq. (5.2). We thus obtain the same strategic behavior as the symmetrized game Eq. (5.4).

We have defined some of the initial conditions that are needed to specify a complete solution to the field equations. Before continuing, it is worth considering the multiplicity of payoffs that are possible, which seemingly represent the same strategic situation. We look at the elementary aspects of *game theory* for example and see that the strategic content of a game in normal form does not change if the payoffs are all multiplied by a common factor. Similarly the strategic content doesn't change if a constant is added to all of the payoff elements. The max-min rule discussed in section 1.4 yields the same equilibrium strategies. If the game is fair, there is no difference between these games. If the game is not fair, the only difference is the size of the payoff, which will be modified by the same multiplicative factor or additive constant that modifies the individual payoffs. The important question is whether this behavior squares with our common sense. It is reasonable to imagine that the strategic choices will in fact be impacted significantly if a game with low stakes is made into a high stakes game. In our *decision process theory*, we in fact expect there to be differences.

The reason for this expectation is that in *decision process theory*, the payoffs are fields that carry energy. The larger the field values the more energy these fields carry. We noted the acceleration flow depends on the inertial and *orientation flux fields*, Eq. (5.6). The acceleration flow is a direct measure of changes to the strategic values. The magnetic components in the co-moving basis play no direct role, whereas the inertial and charge gradient terms do. We thus have at least one difference between our *decision process theory* and *game theory* models that can be put to the test. As we develop the *player fixed frame model* for the prisoner's dilemma, we will study the consequences of different *game values* by changing the initial conditions with additions of constant matrices Eq. (5.10). In the next section we introduce the *code of conduct* and its relationship to inactive strategies.

5.4 *Persistency, variability and code of conduct*

The most general approach to the prisoner's dilemma (section 5.2) is to start with the four active strategies associated with our normal form payoffs Eq. (5.11) and (5.12). To these strategies we add two inactive strategies, one for each of the two prisoners. We use the normal form payoffs plus the appropriate constant matrix $c(v)$, Eq. (5.10) as the initial payoff field value. We use an initial flow value that represents the strategic choice we want to study. For numerical solutions, we specialize to the *player fixed*

frame model that has streamline solutions that can be found using the equations from section 4.5 based on the *quasi-stationary hypothesis*. We expect solutions that are both stationary and non-stationary.

To break out of the prisoner's paradox, we impose a player ***code of conduct*** in which we go from two players to five players, three of which collectively choose a single common active strategy. In these solutions, we maintain the same initial conditions for the payoffs and strategies. Such solutions will have additional persistency that manifests as additional isometries. The method we use to find such solutions is to rotate our frame of reference by a constant amount (*i.e.* an amount independent of space and time). Moreover, we suggested from a preliminary look at the behavior of the acceleration gradient Eq. (5.6) that some, though not all essential features might be seen in these solutions even though they are less general and simpler to study.

Every possible player strategic choice need not be active. For each inactive strategy x, the associated payoff for each player $F^{j}{}_{xb}$ has a form simpler than Eq. (1.73), and provides the payoff in terms of the underlying potentials:

$$F^{j}{}_{xb} = -\partial_b A^{j}_{x} \tag{5.13}$$

This is because none of the metric or orientation potentials can depend on this strategy. From the standpoint of setting initial conditions, we don't see any difference between a single strategy being inactive and none of the strategies being inactive. However, we would expect a difference in the behavior along the *streamlines*. For an inactive strategy, the *streamline* is conserved, Eq. (1.76) extended to the case of a non-zero source (also *Cf.* Table 4-1):

$$\frac{dV_k}{d\tau} = q_\upsilon E_j{}^{\upsilon} + q_\alpha E_j{}^{\alpha} = 0 \tag{5.14}$$

For the *player fixed frame model*, the flow is conserved. This is distinct from the behavior expected for active strategies that will be influenced by the rotational effects of the payoff matrix seen in Eq. (5.5). Multiple numerical examples are provided of this behavior by (Thomas G. H., 2006).

If two strategies $\{x \quad y\}$ are inactive, in addition to the conservation behavior Eq. (5.14) of these strategies along the streamline, there can be no payoff between them:

$$F^{j}{}_{xy} = 0 \tag{5.15}$$

Looking at the payoffs for the prisoner's dilemma, we see no immediate evidence that this is true simultaneously for our initial payoff values Eq. (5.11) and (5.12). There may however be a different basis in which this is true.

We start with a frame in which for each player one direction is specified by *confess* (C) and the other *not confess* (N). An equally complete choice would be the sum (C+N) and difference (C-N) of the strategies. We label the coordinates $\{t,\ \xi_1,\ \xi_2,\ N_2,\ C_2,\ N_1,\ C_1\}$ in our initial *normal-form coordinate basis.* We label $\{\xi_1 \quad \xi_2\}$ the player inactive strategies and label time as t. We make two successive linear transformations starting with:

$$\begin{aligned} s_1 &= {}^{1}\!/_{\sqrt{2}}\left(N_1 - C_1\right) \\ s_2 &= {}^{1}\!/_{\sqrt{2}}\left(N_2 - C_2\right) \\ r_1 &= {}^{1}\!/_{\sqrt{2}}\left(N_1 + C_1\right) \\ r_2 &= {}^{1}\!/_{\sqrt{2}}\left(N_2 + C_2\right) \end{aligned} \tag{5.16}$$

The sum of the strategies for each player, r_1 and r_2, represent how *often* each player plays. They represent the ***player preference scale***. The differences s_1 and s_2 represent the ***player relative preference*** to not confess. In this basis, we still can't choose more than one strategy to be inactive.

Another equivalent set of strategies is the sum r and difference u, leaving all other variables unchanged:

$$\begin{aligned} r &= {}^{1}\!/\!_{\sqrt{2}}\left(r_1 + r_2\right) \\ u &= {}^{1}\!/\!_{\sqrt{2}}\left(r_2 - r_1\right) \end{aligned} \tag{5.17}$$

In this case the resultant payoffs now have a form that is consistent with taking three of the strategies inactive. With the coordinate basis order $\{u \quad r \quad s_1 \quad s_2 \quad t\}$, we have for player 1 the initial payoff matrix:

$$\bar{F}^{1}_{ab} - \bar{c}_{ab}\left(-{}^{9}\!/\!_{10}\right) = \begin{pmatrix} 0 & -{}^{4}\!/\!_{5} & {}^{1}\!/\!_{10}\sqrt{2} & -{}^{9}\!/\!_{10}\sqrt{2} & 0 \\ {}^{4}\!/\!_{5} & 0 & 0 & 0 & 0 \\ -{}^{1}\!/\!_{10}\sqrt{2} & 0 & 0 & 0 & 0 \\ {}^{9}\!/\!_{10}\sqrt{2} & 0 & 0 & 0 & 0 \\ 0 & 0 & 0 & 0 & 0 \end{pmatrix} \tag{5.18}$$

The transformed payoff field for player 2 has a similar structure:

$$\bar{F}^{2}_{ab} - \bar{c}_{ab}\left({}^{9}\!/\!_{10}\right) = \begin{pmatrix} 0 & {}^{4}\!/\!_{5} & {}^{9}\!/\!_{10}\sqrt{2} & -{}^{1}\!/\!_{10}\sqrt{2} & 0 \\ -{}^{4}\!/\!_{5} & 0 & 0 & 0 & 0 \\ -{}^{9}\!/\!_{10}\sqrt{2} & 0 & 0 & 0 & 0 \\ {}^{1}\!/\!_{10}\sqrt{2} & 0 & 0 & 0 & 0 \\ 0 & 0 & 0 & 0 & 0 \end{pmatrix} \tag{5.19}$$

To recover the original form of the payoffs for the prisoner's dilemma we also need to transform the constant value matrix Eq. (5.10):

$$\bar{c}\left(v\right) = \begin{pmatrix} 0 & -2v & 0 & 0 & {}^{2v}\!/\!_{\zeta^0} \\ 2v & 0 & 0 & 0 & 0 \\ 0 & 0 & 0 & 0 & 0 \\ 0 & 0 & 0 & 0 & 0 \\ -{}^{2v}\!/\!_{\zeta^0} & 0 & 0 & 0 & 0 \end{pmatrix} \tag{5.20}$$

Furthermore, the transformation is not specific to the exact form we chose for the prisoner's dilemma. We pick the following payoff based on arbitrary values $\{x \quad y \quad z \quad w\}$:

$$\begin{pmatrix} 0 & z & -w - {}^{1}\!/\!_{2}\left(x - y + z\right) & -w - {}^{1}\!/\!_{2}\left(x + y + z\right) & {}^{w}\!/\!_{\zeta^0} \\ -z & 0 & -w - {}^{1}\!/\!_{2}\left(x - y - z\right) & -w - {}^{1}\!/\!_{2}\left(x + y - z\right) & {}^{w}\!/\!_{\zeta^0} \\ w + {}^{1}\!/\!_{2}\left(x - y + z\right) & w + {}^{1}\!/\!_{2}\left(x - y - z\right) & 0 & y & -{}^{w}\!/\!_{\zeta^0} \\ w + {}^{1}\!/\!_{2}\left(x + y + z\right) & w + {}^{1}\!/\!_{2}\left(x + y - z\right) & -y & 0 & -{}^{w}\!/\!_{\zeta^0} \\ -{}^{w}\!/\!_{\zeta^0} & -{}^{w}\!/\!_{\zeta^0} & {}^{w}\!/\!_{\zeta^0} & {}^{w}\!/\!_{\zeta^0} & 0 \end{pmatrix} \tag{5.21}$$

The transformed payoff is the most general form in which the three strategies $\{r \quad s_1 \quad s_2\}$ can be inactive:

$$\begin{pmatrix} 0 & -2w - x & y\sqrt{2} & -z\sqrt{2} & {}^{2w}\!/\!_{\zeta^0} \\ 2w + x & 0 & 0 & 0 & 0 \\ -y\sqrt{2} & 0 & 0 & 0 & 0 \\ z\sqrt{2} & 0 & 0 & 0 & 0 \\ -{}^{2w}\!/\!_{\zeta^0} & 0 & 0 & 0 & 0 \end{pmatrix} \tag{5.22}$$

We see that the Nash equilibrium is satisfied with $\bar{\zeta}_{Nash} = \{0 \quad 1 \quad -1/\sqrt{2} \quad -1/\sqrt{2} \quad \zeta^0\}$ in all cases but Eq. (5.22). We see that only the first row and first column are non-zero, indicating that we could take some or all of the strategies $\{r \quad s_1 \quad s_2\}$ to be inactive. For Eq. (5.22), we obtain the same Nash equilibrium whenever both $\{y \quad z\}$ are positive and $z = x + y$. We see the possibility that an equilibrium value at a point does not imply an equilibrium value at all points.

To understand inactive strategies better, we elaborate on the meaning of the payoffs that we have found above. The solutions we consider for the prisoner's dilemma reflect a ***symmetric decision process*** and could be a ***just decision process*** in which the ***relative player effort*** u of the prisoners generates a payoff whatever the other strategy is from Eq. (5.21). There are no payoffs that depend purely on the *player relative preferences* $\{s_1 \quad s_2\}$ or ***total player effort*** r. The game theory model assumes that this is true for all time and for all strategic positions. Thus it is as if these strategies play no role. Even if we adopt this stance, we assume only that they are inactive: they still may influence the outcome of the decision indirectly. In this sense we look at the symmetric prisoner's dilemma as being equivalent to a decision process in which there are three additional players controlling the influence of the inactive strategies $\{r \quad s_1 \quad s_2\}$. We note that the general case would diverge from the usual prisoner's dilemma in that it would assume the zero payoffs found above hold only at a single point of space and time.

Our symmetric prisoner's dilemma still may represent a ***utilitarian solution*** or a ***just solution*** depending on the initial flows along the player preferences $\{s_1 \quad s_2\}$. In either case we achieve the effect using a *code of conduct*. A *code of conduct* can just as easily deny rights based on *self-interest* as proffer rights that uphold the *public-interest*. We could also frame a model whose only solutions would be just (exercise 4). Our choice here was based on wanting a model where we could move between these opposite choices as part of our sensitivity analysis of the numerical solutions. Based on these analyses we are able to identify the mechanisms that are needed to support the *just solutions* (*Cf.* section 5.6).

With these caveats, we develop the consequences of the prisoner's dilemma considered as a *player fixed frame model* in which there is a single active strategy $u = 1/\sqrt{2}(r_2 - r_1)$ measuring the ***relative player effort*** of the two prisoners. The *stationary* single strategy solutions we obtain are consistent with (Thomas G. H., 2006), though we extend these solutions to dynamic steady-state solutions. Moreover, the choice of the three inactive strategies is equivalent to a ***code of conduct*** (section 7.2) in which each player will fix the rate at which they will confess. The code of conduct is that each prisoner agrees to treat his strategy difference s_k as inactive. Although each prisoner controls his own difference, we assume that there are various levels of enforcement that hold these strategies inactive. Furthermore, we identify an additional code of conduct by taking the overall ***player scale***, which is the sum of the two active summed strategies $r_1 + r_2$, to be inactive. This strategy is controlled jointly by the two prisoners. Depending on the specifics, we may also envision all three inactive strategies as being controlled jointly. The sole active strategy u that remains reflects the *relative player effort* of the two prisoners. This introduces an effective agent reflecting joint control, which is accountable for the *relative player effort* choice. We suggest the terminology that when this variable is positive, player 2 is the ***aggressor*** and when negative player 1 is the *aggressor*.

In the next section, we start with the initial conditions based on the initial payoff and strategy flows. We demonstrate that we need not choose the initial strategy to be the Nash equilibrium in order to obtain stable solutions to the field equations.

5.5 *Known behaviors*

A consequence of the expanded scope of our *decision process theory* is that we need to specify more behaviors than just payoffs and active strategies. We have introduced inactive player strategies as the mechanism that underlies the notion of a player and payoffs. In addition there are orientation potentials

whose existence and behaviors follow from our *decision process theory*. We set these initial behaviors of the prisoner's dilemma for the *player fixed frame model* with a single active strategy.

We keep in mind the following as we proceed. First, we are looking for solutions to the prisoner's dilemma that have three additional isometries. We are thus justified in calling such solutions *symmetric*. These isometries are associated with a code of conduct the players agree to adhere to. We are also justified in thinking of such solutions as *just*. General solutions to the prisoner's dilemma have much in common with the *utilitarianism* school in ethics (Tavani, 2011), whereas symmetric solutions have more in common with *just utilitarianism*.

Second, we must be mindful of what we mean by initial conditions. Solutions to partial differential equations have unique solutions when the form of the solution is specified on some initial boundary or bounding surface. It may be at an initial point in time or space. If our intent was to predict the future based on a known state of the prisoner's knowledge about each other and the situation, then the initial conditions would be based on time. Our goal here is a little different in that we want to provide an illustrative set of numerical examples. For this reason we consider specifying the system in a state with certain simple properties. For example we "start" the system at a point with zero acceleration, which facilitates our study of whether it stays at that point or not. We shall refer to the behaviors at our "starting" point as the ***known behaviors***.

The third point to keep in mind as we proceed is that the general description of the decision process Eq. (3.5) depends on the strategies we identify as active and inactive in the *normal-form coordinate basis*:

$$d\tau^2 = \gamma_{jk}\left(d\xi^j + A^j_a dx^a\right)\left(d\xi^k + A^k_b dx^b\right) + g_{ab}dx^a dx^b \tag{5.23}$$

The invariant distance τ we term the ***proper time***. We formulate each decision process at the outset assuming that the only inactive strategies are set by player inactive strategies. However we also note that we put all strategies on an equal footing when we use the *holonomic basis* for the strategies:

$$d\tau^2 = \hat{\gamma}_{\mu\nu}dx^\mu dx^\nu \tag{5.24}$$

We can transform from one basis to another, Eq. (1.69) by comparing terms. We now have a third basis that proves insight, which is the ***symmetric normal-form coordinate basis*** whose form is identical to Eq. (5.23) but the inactive strategies now include all the isometries, with a corresponding reduction in the active strategies. We will use the holonomic form Eq. (5.24) as the common ground to relate values from one basis to another.

In this section, we need to specify the known flows, set the values for the orientation potentials for the symmetric prisoner's dilemma, transform these values from the *symmetric normal-form coordinate basis* to the *symmetric co-moving orthonormal coordinate basis* and deal with the specification of inertial effects that have no analogy in game theory. We deal with each of these topics in the following sub-sections.

5.5.1 Known strategic flows

In the *symmetric normal-form coordinate basis*, the initial flow V^μ is specified by the active components V^a determined by the strategies chosen and the inactive components V_j that specify the coupling of the payoffs fields to the flow. Along a streamline, these flow components are the rates of change:

$$V^\mu = \frac{dx^\mu}{d\tau} \tag{5.25}$$

We have normalized the flow to unit length, Eq. (5.8) and Eq. (5.24):

$$\hat{\gamma}_{\mu\nu}\frac{dx^\mu}{d\tau}\frac{dx^\nu}{d\tau} = 1 \tag{5.26}$$

Based on an initial flow direction, there is a natural set of orthonormal vectors that can be constructed. The set aligns *proper time* along the flow direction and constructs vectors transverse to the flow using the Gramm-Schmidt orthogonalization process, starting with the initial strategy directions.

We sketch this process. The first step is to take $E^{a}{}_{o} = V^{a}$ and $E_{jo} = V_{j}$. We then choose the remaining vectors in some order, which we take to be along ξ_1 ξ_2 s_1 s_2 r u. These are independent of the flow, though not in general transverse to the flow. We take a unit direction along the first strategy ξ_1, which defines the direction U_1. We construct a new orthonormal vector that is both orthogonal to the flow and of unit length:

$$E^{\mu}{}_{1} = -\frac{U^{\mu}{}_{1} - U^{\nu}{}_{1}E_{\nu o}E^{\mu}{}_{o}}{\hat{\gamma}_{\mu\lambda}\left(U^{\mu}{}_{1} - U^{\nu}{}_{1}E_{\nu o}E^{\mu}{}_{o}\right)\left(U^{\lambda}{}_{1} - U^{\nu}{}_{1}E_{\nu o}E^{\lambda}{}_{o}\right)} \tag{5.27}$$

We go through each vector and use the same algorithm. Each new vector must be orthogonal to all previous vectors and have unit length. This process can be done in any frame of reference.

The last strategy will be the active *relative player effort strategy*, u. In the *symmetric normal-form coordinate frame*, this strategy is orthogonal to each inactive strategy. In picking the corresponding orthonormal direction υ associated with the *relative player effort*, we therefore can set $E_{j\upsilon} = 0$ for each inactive strategy j.

Since the initial active strategy flows are known, to complete the specification of the flow vector, we need only the magnitude of the time component of the flow m and the player inactive strategy flows. We start the inactive flows at zero. The players are ***uncoupled*** from the decision process. This is not unreasonable if we assume that we start at an equilibrium position $q_\upsilon = 0$. The inactive flows are determined from Eq. (3.64):

$$\partial_\upsilon E_{jo} = -q_\upsilon E_{jo} - 2\omega_\upsilon{}^{\alpha} E_{j\alpha} \tag{5.28}$$

If there is a non-zero charge gradient $\omega_{\upsilon\alpha}$, the player will develop a non-zero coupling away from equilibrium. We think this provides support for the streamline solution choice that the electric field is zero, Eq. (4.76).

Given the initial flow directions and from this the values of the complete *symmetric co-moving orthonormal* set at some initial position, we use Eq. (4.107) to determine the *symmetric co-moving orthonormal frame* at all other positions. These equations provide coupled differential equations in the ***proper relative player effort*** υ and can be uniquely solved once the coefficients in the equations are determined. The coefficients are the orientation potentials, which we deal with next.

5.5.2 Known payoff fields and associated orientation potentials

Given the initial conditions for the *symmetric co-moving orthonormal* vectors, we have the differential equation Eq. (4.107) that determines the inactive components at all other points of space assuming we know the scalar functions for the acceleration q_υ, charge gradients $\omega_{\upsilon\alpha}$, *tidal bond components* $\omega_{\upsilon\alpha\beta}$ and charges e_α. The latter however is not independent based on Eq. (3.69). We solve for the unknown scalars using the field equations Eq. (4.108), (4.109), (4.110), (4.111), (3.69) and (4.78):

$$\begin{aligned}
&\partial_\upsilon \omega^{\upsilon}{}_{\alpha} = 2\omega_{\upsilon\alpha}q^{\upsilon} - \omega^{\upsilon}{}_{\alpha\beta}\omega_{\upsilon}{}^{\beta} + \omega^{\upsilon\beta}{}_{\beta}\omega_{\upsilon\alpha} \\
&\partial_\upsilon \omega^{\upsilon}{}_{\alpha\beta} = \omega^{\upsilon}{}_{\alpha\beta}q_\upsilon + \omega_{\upsilon\gamma}{}^{\gamma}\omega^{\upsilon}{}_{\alpha\beta} + 2\omega_{\upsilon\alpha}\omega^{\upsilon}{}_{\beta} - \kappa\left(p_{\alpha\beta} - ph_{\alpha\beta} + \frac{\mu - p}{n-1}h_{\alpha\beta}\right) \\
&\kappa p^{\upsilon}{}_{\upsilon} = -\omega^{\upsilon\beta}{}_{\beta}q_\upsilon + \omega_{\upsilon\alpha}\omega^{\upsilon\alpha} + \tfrac{1}{2}\omega^{\upsilon\alpha}{}_{\beta}\omega_{\upsilon\alpha}{}^{\beta} - \tfrac{1}{2}\omega_{\upsilon\alpha}{}^{\alpha}\omega^{\upsilon\beta}{}_{\beta} \\
&\partial_\upsilon q^{\upsilon} = q_\upsilon q^{\upsilon} + \omega^{\upsilon\beta}{}_{\beta}q_\upsilon - 2\omega_{\upsilon\alpha}\omega^{\upsilon\alpha} + \kappa\left(\mu + p - \frac{\mu - p}{n-1}\right) \\
&\partial_\upsilon e_\alpha = -q_\upsilon e_\alpha + 2\omega_{\upsilon\alpha} + \omega_{\upsilon\alpha\beta}e^{\beta} \\
&p_{\alpha\upsilon} = 0
\end{aligned} \tag{5.29}$$

We make model assumptions about the inertial components $p_{\alpha\beta}$ and the relationship between energy density μ and pressure p (sub-section 5.5.4). To complete our specification of the numerical problem for the field equations, we have to determine the initial values of the charge gradient and *tidal bond components*. These we show are related to the payoff fields.

To relate the initial values of these orientation potentials to payoffs, we start with the normalized flow Eq. (5.26). We note that this holds in any frame of reference and provides the basis for discussing the prisoner's dilemma in the *normal-form coordinate basis*, the *symmetric normal-form coordinate basis*, the *holonomic basis* or the *symmetric co-moving orthonormal coordinate basis*:

$$\begin{aligned}\hat{\gamma}_{jk} &= \gamma_{jk} \\ \hat{\gamma}_{ja} &= \gamma_{jk}\overline{A}^{k}_{a} \\ \hat{\gamma}_{ab} &= \overline{g}_{ab} + \gamma_{jk}\overline{A}^{j}_{a}\overline{A}^{k}_{b}\end{aligned} \tag{5.30}$$

The metric potentials $\hat{\gamma}_{\mu\nu}$ in the *holonomic basis* tie these different descriptions together. So for example, we have on the left the metric potentials in the *holonomic basis*, whereas on the right we have the potentials that describe behaviors in the *normal-norm coordinate basis*.

In addition to the strategic flows V^{a}, we know the initial behaviors of the payoffs, which are related to the *holonomic metric potentials*. Assuming the transformed basis from section 5.4 and further assuming that the metric potentials are independent of all coordinates except $(u \quad t)$, we relate the metric potentials to the *normal-form coordinate basis potentials*:

$$\begin{aligned}&j,k = \xi_1,\xi_2 \\ &m = r,s_1,s_2 \\ &a,b = u,t \\ &\partial_a\hat{\gamma}_{jm} = \partial_a\gamma_{jk}\overline{A}^{k}_{m} + \gamma_{jk}\partial_a\overline{A}^{k}_{m} = \partial_a\gamma_{jk}\overline{A}^{k}_{m} + \gamma_{jk}\overline{F}^{k}_{am} \\ &\partial_a\hat{\gamma}_{jb} - \partial_b\hat{\gamma}_{ja} = \partial_a\gamma_{jk}\overline{A}^{k}_{b} - \partial_b\gamma_{jk}\overline{A}^{k}_{a} + \gamma_{jk}\overline{F}^{k}_{ab}\end{aligned} \tag{5.31}$$

No result of the theory depends on the initial value of the vector potentials $\overline{A}^{j}_{a} = \overline{A}^{j}_{m} = 0$, so there is no loss in generality setting them to zero; this is a consequence of gauge invariance. Similarly there is no loss in generality in taking the initial metric potentials equal to the Minkowski metric $m_{\mu\nu}$.

We look only for the streamline solutions of section 4.5, which have an initial time derivative of zero. We thus obtain the following:

$$\begin{aligned}\partial_u\hat{\gamma}_{jm} &= m_{jk}\overline{F}^{k}_{um} \\ \partial_t\hat{\gamma}_{jm} &= m_{jk}\overline{F}^{k}_{tm} = 0 \\ \partial_t\hat{\gamma}_{ju} &= 0 \\ \partial_u\hat{\gamma}_{jt} &= m_{jk}\overline{F}^{k}_{ut}\end{aligned} \tag{5.32}$$

Implicit in this description is that the *normal-form coordinate basis* and *co-moving basis* be *aligned* using the Gramm-Schmidt process described above, Eq. (5.27). The *symmetrized normal-form basis* and the *normal-form basis* are aligned, which proves the result. So, in this case initially $t = o = \tau$, time is along the flow (*proper time*) direction and $u = v$, the *relative player effort* is along the *proper active relative player effort strategy* direction. There will be small changes however since the initial flow is not identically along the time direction. For orientation we ignore these small effects but take them into account in our numerical calculations. What is striking is that there are many gradients that are not specified at all, such as $\partial_u\hat{\gamma}_{jk}$. They represent influences that impact the dynamic behaviors but are absent from *game theory* models. We must get better insight into such behaviors.

For the *symmetric normal-form coordinate basis*, we have the same *holonomic metric potentials* $\hat{\gamma}_{\mu\nu}$, which are expressed in a form similar to Eq. (5.30), with the noted differences in what is active and what is inactive:

$$\begin{aligned} &a,b = u,t \\ &j,k = \xi_1,\xi_2,s_1,s_2,r \\ &\hat{\gamma}_{jk} = \gamma_{jk} \\ &\hat{\gamma}_{ja} = \gamma_{jk}A^k{}_a \\ &\hat{\gamma}_{ab} = g_{ab} + \gamma_{jk}A^j{}_a A^k{}_b \end{aligned} \tag{5.33}$$

Of specific interest will be the gradients whose payoff values we know from Eq. (5.32):

$$\begin{aligned} &j,k = \xi_1,\xi_2 \\ &m = r,s_1,s_2 \\ &\partial_u \gamma_{jm} = m_{jk}\bar{F}^k_{um} \\ &\partial_t \gamma_{jm} = m_{jk}\bar{F}^k_{tm} = 0 \\ &\partial_t \hat{\gamma}_{ju} = \gamma_{jk}\partial_t A^k{}_u = 0 \\ &\partial_u \hat{\gamma}_{jt} = \gamma_{jk}F^k{}_{ut} + \gamma_{jm}F^m{}_{ut} = m_{jk}\bar{F}^k_{ut} \Rightarrow F^k{}_{ut} = \bar{F}^k_{ut} \end{aligned} \tag{5.34}$$

We know the initial behaviors of the gradients $\partial_u \gamma_{jm}$ for the indicated restricted set of indices and we know the initial behaviors of $F^k{}_{ut}$ for each prisoner. We don't know the corresponding electric field for the symmetric inactive directions s_1, s_2, r.

5.5.3 Symmetric co-moving frame values

We take the initial behaviors that we have determined and compute the implications in the *symmetric co-moving orthonormal coordinate basis*. We start with the electric field $f^j{}_{ov}$ components from Eq. (4.107), which are determined by the *game values*:

$$f^j{}_{ov} = \left(E^t{}_o E^u{}_v - E^u{}_o E^t{}_v\right)\bar{F}^j_{tu} = 2\left(q_v E^{jo} + \omega_{v\alpha}\left(E^{j\alpha} + e^\alpha E^{jo}\right) + \omega_{v\alpha\beta}e^\alpha E^{j\beta}\right)\left(1 - E^k{}_o E_k{}^o\right) \tag{5.35}$$

To this we add the behavior for $\partial_v \bar{\gamma}_{jm}$ that can be derived from Table 4-1 (Cf. exercise 24 from section 3.11, Eq. (3.85), specialized to the streamline solution), which are set by the initial payoffs for the prisoner's dilemma:

$$\partial_v \gamma_{jm} = m_{jk}E^u{}_v \bar{F}^k_{um} = -2q_v E_{jo}E_{mo} - 2\omega_{v\alpha}\left(E_j{}^\alpha E_{mo} + E_{jo}E_m{}^\alpha\right) - 2\omega_{v\alpha\beta}E_j{}^\alpha E_m{}^\beta \tag{5.36}$$

These two behaviors depend on the acceleration q_v along the *relative player effort* direction. To focus on the possibility of other equilibrium behaviors, we assume that the initial acceleration is zero. To get a rough idea of what is determined, we recall that we align the co-moving frame so that prisoner j is along co-moving direction α_j and assume the initial prisoner flows are zero $E_{jo} = 0$. The latter determine the initial charges, which we are taking as neutral or zero.

With these approximations, we see more clearly what is determined. From the *game value* of the prisoner's dilemma, Eq. (5.35) we determine the charge gradient:

$$\begin{aligned} &j = \xi_1,\xi_2 \\ &\omega_v{}^{\alpha_j} \cong \tfrac{1}{2}\bar{F}^j_{tu} \end{aligned} \tag{5.37}$$

We determine the charge gradient because we have assumed the electric field components $\theta_{v\alpha} = 0$ are zero in order to meet the conditions for the streamline solutions. Given the charge gradient, from the

payoffs of the prisoner's dilemma, Eq. (5.36) we determine the *tidal bond components* that lie along the mixed axes of the inactive player directions and the equivalent player directions:

$$\begin{aligned} &j,k = \xi_1, \xi_2 \\ &m = r, s_1, s_2 \\ &\omega_{\upsilon_u \alpha_j \beta_m} \cong \tfrac{1}{2} \bar{F}^{j}_{tu} E_{mo} - \tfrac{1}{2} m_{jk} F^{k}_{um} \end{aligned} \tag{5.38}$$

In performing the numerical analysis, we use the initial transformation matrix values and Eq. (5.35) and (5.36). There are additional components that we have not determined.

Among the many components not determined are the player components of the *tidal bond* matrix:

$$\begin{aligned} &j,k = \xi_1, \xi_2 \\ &\partial_u \bar{\gamma}_{jk} \cong -2\omega_{\upsilon_u \alpha_j \beta_k} \end{aligned} \tag{5.39}$$

The mixed term is an example of influence of one prisoner on the other that is not part of any payoff matrix. Our strategy in general is to set these new terms to zero unless there are clear reasons for not doing so. At a later time the strategy is to do a sensitivity analysis on these assumptions.

For these mixed terms, there may in fact be reasons not to set them all to zero. One such reason that comes into play is the requirement that the pressure, Eq. (4.110), be positive:

$$\kappa p^{\upsilon}{}_{\upsilon} = -\omega^{\upsilon\beta}{}_{\beta} q_{\upsilon} + \omega_{\upsilon\alpha} \omega^{\upsilon\alpha} + \tfrac{1}{2} \omega^{\upsilon\alpha}{}_{\beta} \omega_{\upsilon\alpha}{}^{\beta} - \tfrac{1}{2} \omega_{\upsilon\alpha}{}^{\alpha} \omega^{\upsilon\beta}{}_{\beta} \tag{5.40}$$

We take the initial acceleration to be zero. We must impose constraints on the unknown compression and charge gradient components in order to insure that this pressure component be positive. Our initial approach will be to use the diagonal components of Eq. (5.39) to accomplish this. We intend to investigate similarly the effects of all undetermined components on the dynamic behavior as they provide valuable insight into the dynamic mechanisms.

5.5.4 Numerical values and inertial effects

The numerical results in this chapter will be based on the following choice for the unit flow with components $\{t,\ \xi_1,\ \xi_2,\ N_2,\ C_2,\ N_1,\ C_1\}$:

$$V^{\mu} = \{1.061 \quad 0. \quad 0. \quad 0.2500 \quad 0. \quad 0.2500 \quad 0.\} \tag{5.41}$$

In the *symmetric normal-form transformed frame* $\{t,\ \xi_1,\ \xi_2,\ s_1,\ s_2,\ r,\ u\}$:

$$\bar{V}^{\mu} = \{1.061 \quad 0. \quad 0. \quad 0.1768 \quad 0.1768 \quad 0.2500 \quad 0.\} \tag{5.42}$$

With these values, for the inactive space $\{\xi_1 \quad \xi_2 \quad s_1 \quad s_2 \quad r\}$ the *charge gradient* and *tidal bond* components are chosen to agree with the *game value* Eq. (5.35) and player payoffs Eq. (5.36) using a $\beta = \tfrac{1}{3}$, which leads to a decision mass of $m = 4$ and hence $\zeta^0 = 4.243\ldots$:

$$\begin{aligned} \omega_{\upsilon\alpha} &= \{-0.1871 \quad 0.1871 \quad 0. \quad 0. \quad 0.\} \\ \omega_{\upsilon\alpha\beta} &= \begin{pmatrix} x_1 & 0. & 0.03706 & -0.6607 & 0.4660 \\ 0. & x_2 & 0.6593 & -0.05706 & -0.4660 \\ 0.03706 & 0.6593 & x_3 & 0. & 0. \\ -0.6607 & -0.05706 & 0. & x_3 & 0. \\ 0.4660 & -0.4660 & 0. & 0. & x_3 \end{pmatrix} \end{aligned} \tag{5.43}$$

We arbitrarily set all the remaining charge gradient and *tidal bond* components to zero with the exception of the diagonal components labeled $\{x_1 \quad x_2 \quad x_3\}$. We distinguish between prisoner 1, prisoner 2 and the remaining inactive dimension. The pressure component Eq. (5.40), with units $\kappa = 1$, is a function of three unknowns (Figure 5-1):

$$p^{\upsilon}{}_{\upsilon} = -1.2400 + x_1 x_2 + 3x_1 x_3 + 3x_2 x_3 + 3x_3{}^2 \tag{5.44}$$

It is clear that we must choose values of these unknowns that are large enough or the pressure will be negative.

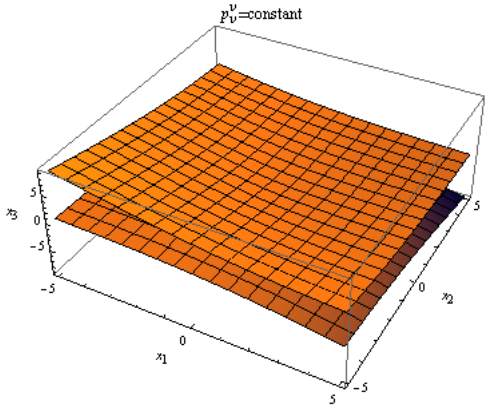

Figure 5-1: Surfaces of constant $p^{\nu}{}_{\nu} = 1.0$ in the parameter space

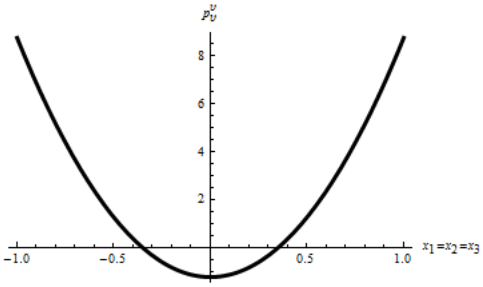

Figure 5-2: Pressure $p^{\nu}{}_{\nu}$

There are two disconnected surfaces, which are illustrated when all three parameters are equal, $x_1 = x_2 = x_3$ (Figure 5-2). For our numerical work, we pick a pressure component $p^{\nu}{}_{\nu} = 1$, which occurs when all three parameters are equal to $x_1 = 1.497$.

We can pick a value in which the pressure is uniformly zero. However the gradient of the acceleration $\partial_{\nu} q^{\nu}$ does not vanish since it is equal to the vorticity squared, Eq. (5.29). A non-zero inertial acceleration implies the existence of an inertial stress or pressure. The pressure changes value at other strategic points.

There are important implications to our need for a non-zero pressure. For a Nash equilibrium, this would not be necessary. Our choice of a non-Nash equilibrium solution requires the existence of inertial pressure to support the stability of the solution with a non-trivial *code of conduct*. Thus we obtain new types of stabilities at the cost of requiring sufficient forces to support them. The *code of conduct* requires additional support in the form of inertial contributions. We shall see that some of these inertial contributions appear as gravitational effects pulling behaviors towards areas where there is already a concentration of inertia.

There are a number of parameters associated with the pressure $p_{\alpha\beta}$, $p_{\nu\alpha}$ and energy density μ that we have not yet specified. These represent significant effects that are not addressed by the concepts of payoffs and strategies. We make the following provisional choice that the pressure and energy density are analogous to a perfect homogeneous fluid:

$$\begin{aligned} p_{\alpha\beta} &= ph_{\alpha\beta} \\ p_{\nu\nu} &= ph_{\nu\nu} \\ p_{\nu\alpha} &= ph_{\nu\alpha} = 0 \end{aligned} \tag{5.45}$$

The homogeneity of the fluid is expressed as:

$$\mu = \alpha p \tag{5.46}$$

The ***resiliency*** α is a measure of internal energy, which in general should be larger than unity. For our model calculations we take $\alpha = 5$.

We have specified a complete set of initial behaviors from which a unique solution to the scalar field equations Table 4-4, Table 4-5 and Table 4-6 can be obtained. Given the scalar fields, we can then obtain the inactive and active transformations Table 4-1. In practice we carry out the solution for these quantities simultaneously as coupled differential equations. We present the stresses, strains and *vorticity* turns that result from our *decision process theory* in the next sections using the software *Mathematica* (Wolfram, 1992). Dynamic behaviors will be introduced in section 5.9 and subsequent sections. They rely on the same scalar solutions, extended to include non-stationary active strategies, Eq. (4.112).

5.6 *Inertial stress behaviors*

In this section we show that inertial effects represented by the stress tensor are needed to support solutions to the prisoner's dilemma in which the prisoner's cooperate for their common good, their ***public-interest***. Such effects are shown not to be needed to support solutions in which players operate only on their ***self-interest***. These results provide important insight into the decision making process. The inertial effects are needed to resolve the paradox of the prisoner's dilemma. More generally they lend support to the importance of contracts (section 7.2) as the necessary ingredient for the ***invisible hand*** (Smith, 1776) that is implicit in game theory arguments.

In *decision process theory*, we identify both the forces that pull the system together as well as the forces that push the system apart. In this section we demonstrate that ***inertia*** generates an attractive force that brings things together. It also generates an opposite force, which is a consequence of energy being concentrated generating stress (pressure). We demonstrate that we can engineer *structurally stable* behaviors by insuring that there is sufficient inertia to generate attractive forces to pull the system together and overcome any destabilizing forces. What is the source of this inertia? We suggest it is the rules of the game, the agreement to adhere to certain standards, to a *code of conduct*.

We turn now to the numerical results based on the known conditions, section 5.5. We view the prisoner's dilemma decision process as one that repeats. It is a set of plays in which each prisoner can wager but only the difference in wagers u is an active strategy. Each prisoner learns from the previous plays and so each prisoner comes to a conclusion about what to do next. The decisions are more complex than simply having a payoff matrix, though that is part of their considerations. In addition there is the ***inertial acceleration*** q^v that is determined by the energy density and stress tensor, the ***strains*** and their gradient variation as a function of the active strategy. Finally there is the ***vorticity***: the turns, twists, rotations that are possible without generating strains. We think of fixed point behavior as associated with a point at which there is zero acceleration. The question of ***structural stability*** is then whether the system as a whole would move towards, away or around this point if the restrictions based on the *quasi-stationary hypothesis* were removed.

5.6.1 Model results

The general *decision process theory* Table 4-6 identifies in Eq. (2.42), the change in inertial acceleration q^v, which is also the acceleration determined by the source energy momentum tensor. We made the assumption that the pressure was initially non-zero. Based on the known behaviors (section 5.5), the field equations lead to a pressure that is peaked at the origin, $v = 0$, Figure 5-3. We emphasize that this result is a consequence of the field equations and the known conditions.

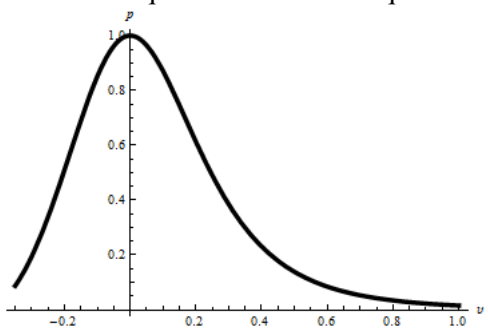

Figure 5-3: Pressure p versus v

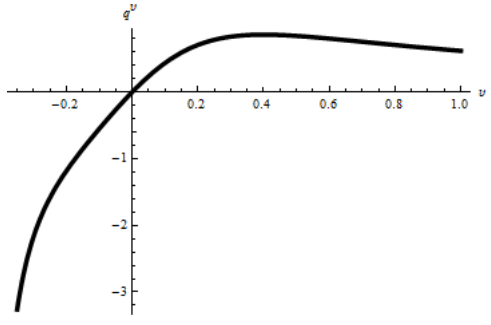

Figure 5-4: The inertial acceleration q^v versus v

Our *stationary* solution for pressure demonstrates its tendency to bunch around the origin. We note that the pressure is not symmetric, but drops off more dramatically on the left (prisoner 1 is more engaged) than on the right (prisoner 2 is more engaged). The origin of the asymmetry is that there are two possible solutions of pressure in Figure 5-2 for any given positive pressure. Our treatment is symmetric in

the sense that there is another solution $x_1 = -1.497$ that is the mirror of Figure 5-3. Nevertheless each solution demonstrates an asymmetry.

We are not surprised that the pressure has a maximum at the origin. The assumption that the origin was a point of zero acceleration defines the position of the peak for pressure. Moreover, since the energy density is proportional to the pressure, it too peaks at the origin and has the same shape. The consequence of the strong pressure peak at the origin is that the acceleration Figure 5-4, which is roughly proportional to minus the gradient of the pressure (Eq. (4.53)) will be positive when prisoner 2 is more engaged (on the right) and negative when prisoner 1 is more engaged (on the left).

If we think of the inertial acceleration as being balanced by the gradient of an ***inertial potential*** $-q$ that represents the attraction that decisions tend to follow previous decisions, then the potential should represent an attractive well, Figure 5-5:

$$q_\upsilon = \partial_\upsilon q \tag{5.47}$$

Inertia produces many effects, one of which is this one describing acceleration. It is analogous to the physics potential in that the negative gradient of the potential is the force, which is proportional to the acceleration. In the next section (section 5.7.1) we shall see that inertia determines the volume effects. When we compute the time component of the metric potential g_{tt} (section 5.9), we shall see that the charge density determines the initial shape. The charge density is indirectly determined by the inertial effects. There are many types of effects, clearly indicating that the inertial effects are not scalar but tensor forces.

At this point we observe that in the *co-moving frame*, the spatial components of the flow are zero, which leads us to Eq. (5.47). This equation and the shape of the potential well Figure 5-5, support our argument that inertial effects induce stability. We believe this is a crucial aspect of decision making when there is a non-trivial *code of conduct*. Decisions will collect together; where they collect creates an equilibrium point. Because they collect they attract subsequent decisions towards the same point in a way analogous to gravitational attraction. This equilibrium point is determined by the *code of conduct*, not by considerations of *utility, self-interest*, or even *public-interest*.

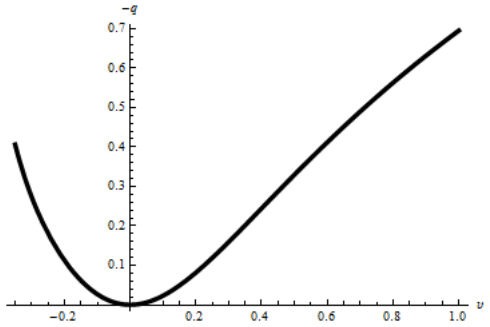

Figure 5-5: Inertial potential $-q$

In *decision process theory*, the attribute that the pressure bunches around the origin does not hold in general. For these symmetric solutions of the prisoner's dilemma, it holds for initial pressures down to a critical pressure $p_c = 0.02693\ldots$ defined as the point at which the acceleration gradient vanishes, which is proportional to the scalar formed from the charge gradients, $\omega_{\upsilon\alpha}\omega^{\upsilon\alpha}$.

Below this pressure the equilibrium point moves away from the symmetric center. The cause is traced to the presence of the centrifugal effect of $\omega_{\upsilon\alpha}$. We investigate this in more detail, since this provides an understanding of the source of stable behaviors.

5.6.2 Sensitivity Analysis

We do a sensitivity analysis by considering several cases each with an initial pressure of 0.01 that is below the critical pressure. We vary the input flow keeping the inertia fixed at the model value of 4. We call the flow in which both prisoners choose not to confess the ***common good*** solution. The Nash equilibrium flow where both prisoners confess we call the ***Nash solution***. We consider these two solutions, with and without a non-zero *game value*.

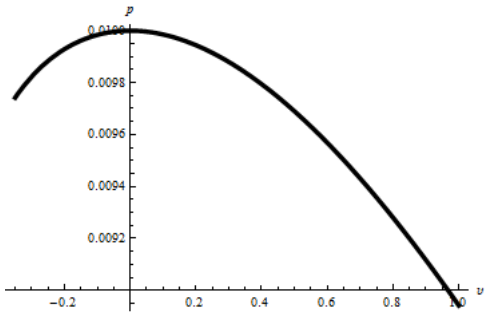

Figure 5-6: Pressure for *Nash solution* with no *game value*

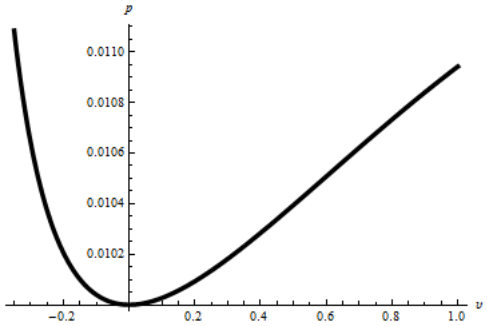

Figure 5-7: Pressure for *common good* solution with no *game value*

For the Nash solution, the shape of the pressure for zero *game value*, Figure 5-6, has a peak at the origin. This demonstrates that nothing prevents the bunching of the energy density and pressure around zero, because the Nash solution has charge gradients $\omega_{v\alpha}$ that are almost identically zero when there is no *game value*. We find that the Nash solution is *structurally stable* for zero *game value* in the simple sense of attraction.

In contrast, the pressure for the *common good* solution, Eq. (5.41), has a minimum at the origin, Figure 5-7. It demonstrates that with the same assumptions and no *game value*, the charge gradients lead to a stable solution based on the pressure gradient. Again, extra energy is expended to insure the *stationary* behavior. The corresponding potential well Figure 5-5 turns into a potential mountain. We conclude that there is not enough inertial mass to balance out the centrifugal effect ascribed to the game, Figure 5-8, though there is sufficient pressure gradient. We thus find evidence that this solution is not *structurally stable*.

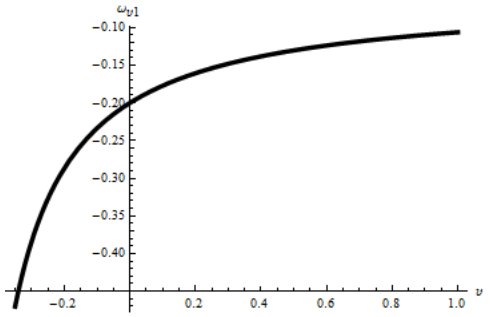

Figure 5-8: Vorticity $\omega_{v\alpha}(v)$ for player 1 for *common good* solution with no *game value*

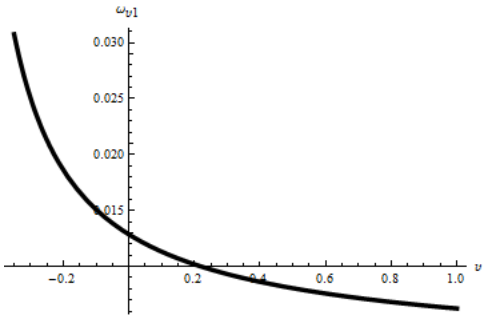

Figure 5-9: Vorticity $\omega_{v\alpha}(v)$ for player 1 for *Nash solution* with *game value*

We thus agree with the assessment that the *common good* solution is possibly less *structurally stable* in the absence of inertial effects. However we showed that with sufficient initial energy density, the instability can be overcome, Figure 5-3. The source of the sign change is clearly seen in Eq. (5.6). Whenever there is a charge gradient, the initial pressure has to be large enough to overcome the effects or the origin will be unstable.

There are other sources to a non-zero charge gradient, one of which is the existence of a non-zero *game value*. For the *Nash solution*, the charge gradient Figure 5-9, is about an order of magnitude smaller than the effect due to the *common good* solution. Nevertheless it is there and the pressure has to be large enough to overcome this. The critical pressure here is much smaller. Although for an initial pressure of 0.01, the pressure has a maximum at the origin, for a pressure sufficiently small, the maximum turns into a minimum.

As the pressure increases, the shape of the potential well Φ, Eq. (5.47), narrows. In other words, we increase the stability. As the pressure decreases towards the critical pressure, we decrease the stability. There are other inertial parameters, the inactive component stresses $p_{\alpha\beta}$ and $p_{\nu\alpha}$ and the energy density $\mu = \alpha p$, which further refine the shape of the potential well. The critical pressure depends not only on the initial (average) pressure p but on the resilience α. For now we don't have sufficient information to further refine our understanding of these effects and so leave them to a future study.

In this model case, we see the consequences of $\theta_{\nu\alpha} = 0$. With this assumption, we see that a non-zero *game value* induces instability because it leads to a non-zero value of the charge gradient. If we have a decision process with a very high *game value*, this process will be intrinsically more unstable than a process with a smaller value. We associate a very high *game value* with high stakes and high risk. This is less stable than a small *game value*.

This completes our sensitivity analysis and we return to the features of the model defined by the parameters of section 5.5. Our conclusion from this section is that when we are sufficiently above the critical pressure, the inertial energy density provides *structural stability* that counters two potential destabilizing effects: a non-zero value for the game and any flow that is not a Nash equilibrium solution. We investigate metrical behaviors of the solution in the next section.

5.7 *Strain behaviors*

It is not universally accepted that human behavior is subject to the same quantitative discipline that has been applied to the physical sciences. However, the game theory of (Von Neumann & Morgenstern, 1944) is built on this premise. These authors argued that utilities determine the payoffs and are not only ordinal (preferences can be ordered) but cardinal (numerical values can be assigned in a meaningful way). We also believe that numerical measures must be part of *decision process theory*. We believe that utilities can be meaningfully defined that are more than a mere ordering of preferences but a way to distinguish what strategies are near or far from each other. We go beyond *game theory* by requiring that utilities are convertible (section 7.7), which leads us to concepts of space and time that are non-Newtonian.

We make the distinction, as does Einstein in his theory of relativity, between the position of points in space and their distance. The positions of points represent the location of strategic choices in space and time. In a mathematical sense these points have a fixed place in the topology of space and time. A topology provides the concept of what it means to be neighbors but is not sufficient to determine the concept of distance. The existence of a measure for distance requires a physical field that provides the ***connection*** between points in space. This connection provides additional structure to the topology. It carries energy and momentum; it is affected by other physical fields and may change in time and vary in space. The connection is part of the physical world distinct from the topological backdrop. The connection is part of the overall schema that allows utilities to be convertible.

In the physical world, the connection between points is carried out with yardsticks and clocks. In decision processes metrical measures survive that derive from these basic yardsticks and clocks that allow us to quantify choices. We demonstrate this in our theory with the prisoner's dilemma as the teaching example. In the last section we focused on the inertial stresses that arise in the theory. We showed that inertia provides a fundamental mechanism for endowing the system with energy density and pressure, which is the average of the diagonal components of stress.

We use the word ***stress*** in a way analogous to physical theories to represent the forces present. An independent concept is the idea of ***strain***, which highlights the effect on the geometric configurations that measures displacements of the system in space and time. A bridge undergoes stress when a heavy object goes across it. The stress generates strain as evidenced by parts of the bridge that move as a consequence. The strains are in response to the stresses. The notion of strain makes sense for decision processes because changes in the strategy configuration of the system are observable, distinguishable and measurable. In this section and the next we demonstrate that the Electromagnetic field behaviors Table 4-4 and tidal behaviors Table 4-5 define not only the strains such as $\omega_{\nu\alpha\beta}$ associated with movement

along the active direction υ, but through the coordinate transformations they define the metric. The inactive metric components γ_{jk} will make precise the notion of cardinality. In this section, we explore the properties of the strains in the inactive space.

Our numerical work is presented based on expanding the *tidal bond* component $\omega_{\upsilon\alpha\beta}$ into a ***bond compression coefficient*** Θ_υ and ***bond shear components*** $\sigma_{\upsilon\alpha\beta}$:

$$\begin{aligned}\Theta_\upsilon &= h^{\alpha\beta}\omega_{\upsilon\alpha\beta}\\ n_i &= h^{\alpha}{}_{\alpha}\\ \sigma_{\upsilon\alpha\beta} &= \omega_{\upsilon\alpha\beta} - \frac{\Theta_\upsilon}{n_i}h_{\alpha\beta}\end{aligned} \tag{5.48}$$

This decomposition is not only a standard way of analyzing the properties of a symmetric matrix, but has been used to understand the complex field equations of Einstein (Hawking & Ellis, 1973). Any such matrix can be thought of as an operator that transforms the shape of a small cube; since the matrix changes as a function of the active strategy, the shape of the small cube will also change as a function of position. The two of changes correspond to these distinctions.

We can use these ideas to characterize the volume of the cube. The *bond compression* coefficient leads to a change in the volume V:

$$\partial_\upsilon V = \Theta_\upsilon V \tag{5.49}$$

The *bond shear* components leave the volume unchanged but distort the shape of the cube by sliding a face of the cube parallel to one of the other faces in such a way that the volume does not change. It may help to think of a cube of Jell-O as something with a fixed volume and consider different distortions to this. These ideas give a physical picture of the strategic strains on a small cube that is moved along an active strategy direction in the *co-moving frame*.

5.7.1 Compression results

For our streamline solutions of the prisoner's dilemma, we obtain the following equation (*Cf.* exercise 7) demonstrating the close relationship between the stress (pressure) and the strain (compression):

$$\partial_\upsilon\Theta^\upsilon = \Theta_\upsilon\Theta^\upsilon + \Theta^\upsilon q_\upsilon + 2\omega_{\upsilon\alpha}\omega^{\upsilon\alpha} - \kappa\left(\mu - p^\upsilon{}_\upsilon\right) \tag{5.50}$$

In the absence of charge gradients, such as we saw above for the *Nash solution* with no *game value*, the *bond compression* depends only on the energy density, acceleration and stress. For our numerical solution of the prisoner's dilemma with the initial conditions, Eq. (5.35) and (5.36), which gives $\Theta^\upsilon(0) = 2.366$, this shape of the *bond compression* (Figure 5-10) is modified only slightly by the charge gradients.

The *bond compression* gives direct evidence of changes in the configuration as a consequence of the energy density and active stress component. If we move a unit cube in the five inactive dimensions along the active strategy, we find that the volume changes as it moves left or right (Figure 5-11). In particular we see that the size of the box goes to zero as we go further left in the direction in which prisoner 1 is more engaged. As we go to the right, the size of the box becomes constant. The asymmetry of the volume corresponds to the asymmetry noted earlier about the shape of the pressure (sub-section 5.6.1). For our numerical example, we have chosen to focus on solutions in which prisoner 2 is typically more engaged.

The idea that the unit of measure changes depending on where we are, illustrates that in *decision process theory*, the concept of space and its ordinal properties are distinct from the concept of distance and its cardinal properties.

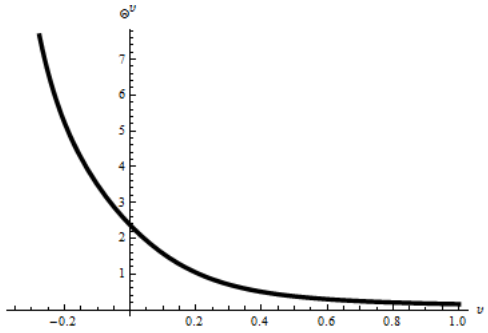

Figure 5-10: The bond compression coefficient $\Theta(\upsilon)=\omega^{\upsilon\alpha}{}_{\alpha}(\upsilon)$

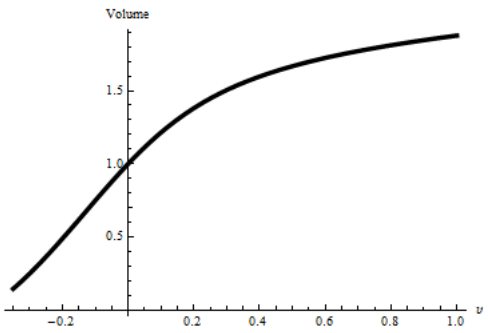

Figure 5-11: Bond compression volume as a function of strategy υ

5.7.2 Shear results

The initial sources of strain are the initial payoffs, Eq. (5.38). In addition to the *bond compression*, these strains generate what we characterize as *bond shear* in which the shape changes without rotation but the volume remains the same. To simplify the interpretation of the numerical results, the equation for the shear can be written in a reduced form similar to exercise 10, which is simpler for the single strategy models with the streamline solution:

$$\begin{aligned}&\sigma^{\upsilon}{}_{\alpha\beta}=\Gamma^{\upsilon}\bar{\sigma}_{\alpha\beta}\\&\partial_{\upsilon}\Gamma^{\upsilon}=(q_{\upsilon}+\Theta_{\upsilon})\Gamma^{\upsilon}\\&\Gamma^{\upsilon}\partial_{\upsilon}\bar{\sigma}_{\alpha\beta}=2\omega_{\upsilon\alpha}\omega^{\upsilon}{}_{\beta}-{}^{2}/_{n_i}\,h_{\alpha\beta}\omega_{\upsilon\gamma}\omega^{\upsilon\gamma}-\kappa\left(p_{\alpha\beta}-{}^{1}/_{n_i}\,h_{\alpha\beta}p^{\gamma}{}_{\gamma}\right)\end{aligned}\qquad(5.51)$$

The factor Γ^{υ}, (see Figure 5-12), depends only on the inertial terms. For the single strategy models, we make no assumption about the form of the stress such as Eq. (5.69). For the case of the numerical example with a perfect fluid, the reduced shear simplifies further:

$$\Gamma^{\upsilon}\partial_{\upsilon}\bar{\sigma}_{\alpha\beta}=2\omega_{\upsilon\alpha}\omega^{\upsilon}{}_{\beta}-\frac{2h_{\alpha\beta}\omega_{\upsilon\gamma}\omega^{\upsilon\gamma}}{n-1}\qquad(5.52)$$

The reduced shear depends on the inertial factors only through the shape factor Γ^{υ}. In particular, when the charge gradients vanish, the reduced shear is constant. According to exercise 10, this also occurs if we make the special choice for the stress, Eq. (5.69).

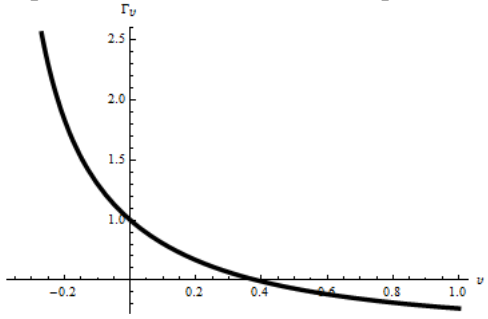

Figure 5-12: Shape factor $\Gamma_{\upsilon}(\upsilon)$ normalized to unity at the origin

For our choice of parameters of the prisoner's dilemma, and with pressure components for an ideal fluid, the charge gradients are small and so the reduced shear is approximately constant (see for example Figure 5-13). Note that the addition of non-ideal stresses $p_{\alpha\beta}$ and $p_{\upsilon\upsilon}$, Eq. (5.51), can change this.

The initial conditions set the initial value of the *bond shear* $\sigma_{\upsilon\alpha\beta}(\upsilon)$ and reduced shear at zero *relative player effort*, Eq. (5.48):

$$\bar{\sigma}_{\alpha\beta}(0)=\sigma_{\upsilon\alpha\beta}(0)=\begin{pmatrix}0 & 0. & 0.03706 & -0.6607 & 0.4660\\ 0. & 0 & 0.6592 & -0.05706 & -0.4660\\ 0.03706 & 0.6592 & 0 & 0. & 0.\\ -0.6607 & -0.05706 & 0. & 0 & 0.\\ 0.4660 & -0.4660 & 0. & 0. & 0\end{pmatrix} \tag{5.53}$$

The off-diagonal elements can be expected to change slowly and represent the payoffs for the prisoner's dilemma as viewed in the effective process in which there are five players and a single active strategy. The payoff values change due to the field equations, so for example at $\upsilon=0.1$ we have:

$$\bar{\sigma}_{\alpha\beta}(\upsilon=0.1)=\begin{pmatrix}0.0039 & -0.0051 & 0.0369 & -0.6609 & 0.4664\\ -0.0051 & 0.0039 & 0.6594 & -0.0569 & -0.4662\\ 0.0369 & 0.6594 & -0.0026. & 0. & 0.\\ -0.6609 & -0.0569 & 0. & -0.0026 & 0.\\ 0.4664 & -0.4662 & 0. & 0. & -0.0026\end{pmatrix} \tag{5.54}$$

One measure of the shear effects is $\bar{\sigma}_{\alpha\beta}\bar{\sigma}^{\alpha\beta}$. It has a maximum at the origin and is roughly constant over the whole range. In addition, shear effects lead to changes in the payoff tensor. In other words, due to successive plays of the decision process, each prisoner adjusts his choice. For steady state behaviors, this will manifest itself as a spatial dependence. For the values chosen here for the prisoner's dilemma, the changes are primarily those due to the change in shape, Figure 5-12, as opposed to changes in the value of the reduced shear, such as Figure 5-13.

There are 14 independent *bond shear* components, of which six we have identified as being related to the payoffs of the prisoner's dilemma. That means there are eight components that measure something new, something that directly relates to the strain configurations that result from the assumed stress. We pick as an interesting example, the mixed component $\bar{\sigma}_{\xi_1\xi_2}$ between the two prisoners, Figure 5-14. We think of the prisoners as interacting only by means of their respective payoffs. However, *decision process theory* provides influence through other means, such as through the *bond shear* components $\bar{\sigma}_{\xi_1\xi_2}(\upsilon)$, Eq. (5.54). Though zero at zero *relative player effort*, it shows a small but non-zero effect at other values of *relative player effort*.

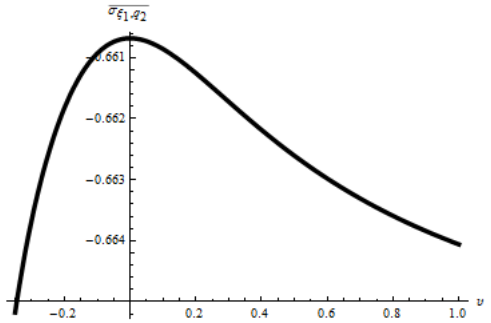

Figure 5-13: Reduced *bond shear* $\bar{\sigma}_{\xi_1 q_2}(\upsilon)$

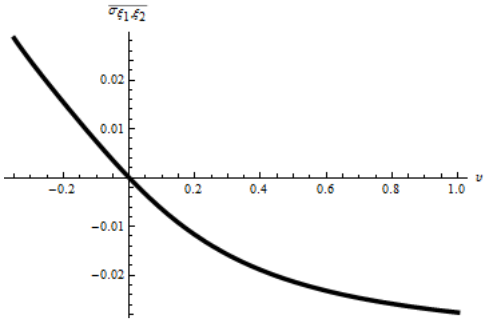

Figure 5-14: Reduced *bond shear* $\bar{\sigma}_{\xi_1\xi_2}(\upsilon)$

5.7.3 Charge gradient results

In addition to *bond shear and compression*, we have tidal charge gradients. The initial charge gradients for prisoner 1 and 2 are set by the *game values*, Eq. (5.37) and the remaining values are set to zero. These initial values in particular determine the tidal charge gradients $\omega_{\upsilon\alpha}$, Figure 5-15. The color

code is that blue, red, green, yellow and purple represent α that are in the initial directions $\{\xi_1 \quad \xi_2 \quad s_1 \quad s_2 \quad r\}$ in the sense of the orthogonalization process described in section 5.5. By assumption only the prisoner's charge gradients along $\{\xi_1 \quad \xi_2\}$ are non-zero at zero *relative player effort*. We have noted that the non-zero charge gradients strongly influence the inertial properties of the acceleration q^{υ}, Eq. (5.6) as well as the *bond shear* Eq. (5.52). From Figure 5-15, we see the effects are particularly strong when prisoner 1 is more engaged, $\upsilon < 0$.

We see from these examples that *stationary* behavior results from strains that, under special conditions, exactly cancel each other. Just as in mechanical engineering, we conclude that forces lead to dynamic behaviors. Stresses lead to strains and hence changes in configurations. Changes in configuration can be minor or catastrophic. We gain insight into those stresses from an analysis of the *stationary* behaviors. In section 5.6, we identified that the forces based on the payoff behavior exist side by side with inertial forces that are significant contributors to equilibrium behaviors. In this section we see that stresses induce strains in the configuration of the system. These strains determine the size of the yardstick by which one measures how near or how far apart two strategic choices are. In this way we capture the variable nature of utility and deal with how to convert the measure of utility from one point in space time to another. In the next section, we analyze the persistent behaviors that result from these stresses and strains and determine the *symmetric normal-form coordinate basis* metric potentials that result.

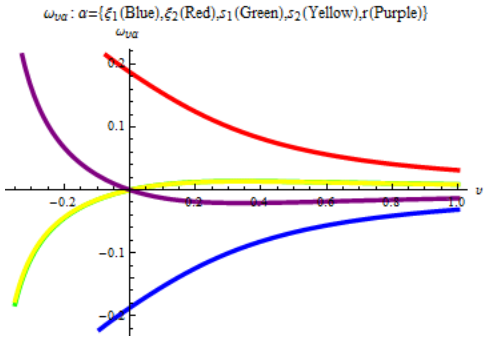

Figure 5-15: Charge gradient field $\omega_{\upsilon\alpha}(\upsilon)$ in the co-moving frame

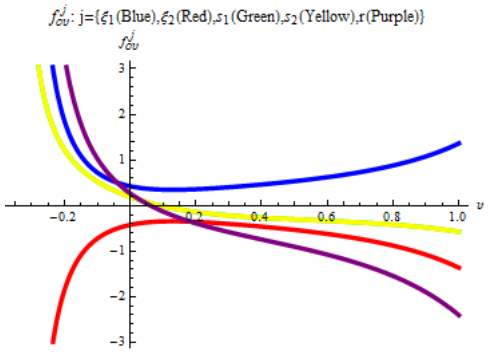

Figure 5-16: Electric field $f^{j}{}_{o\upsilon}(\upsilon)$ in the co-moving frame

5.8 *Persistent behaviors*

Persistent behaviors, Table 4-1, reflect the basic nature of a *player* or *agent* as defined in chapter 3. The notion of persistence comes from the ***metric*** and the concept of ***isometry.*** A metric is the measure of distance between neighboring points, Eq. (1.48). In the last section we highlighted aspects of our theoretical foundation that require the measure between points to change. In general, any transformation of coordinates will cause such a change. However there may be special transformations that leave the metric components unchanged: an *isometry* is a transformation of coordinates that leaves the metric components unchanged.

Our notion of *player* (agent, prisoner, etc.) is based on the existence of an associated *isometry*. We recall that for each player or agent, the *isometry* is defined by the existence of a vector field K^{μ} satisfying the Killing relationship Eq. (3.22). Equivalently, there is an associated dimension ξ^{j} and a *holonomic frame* in which all metric components are independent of this dimension. We showed that the *persistency components* $E_j^{\alpha} \quad E_j^{o} \quad E_j^{\upsilon}$, Eq. (3.61), are in fact the components of such a Killing vector in the co-moving frame. The behaviors of these components in the *co-moving frame* completely characterize the persistency of that player including the inactive metric that is the measure of distance in the inactive space:

$$\gamma_{jk} = E_j{}^o E_k{}^o + E_j{}^\alpha E_k{}^\beta h_{\alpha\beta} \tag{5.55}$$

There are three categories to consider: the inactive behaviors $E_j{}^\alpha$, the active behaviors along the flow $E_j{}^o$ and the active behaviors along the active strategy $E_j{}^\upsilon$. In the *player fixed frame model* the latter components are zero, $E_j{}^\upsilon = 0$. In this section, we analyze the non-zero components for the prisoner's dilemma.

The initial behavior of the *persistency components* result from the initial flows and from the initial orthonormal set described by the Gramm-Schmidt process, section 5.5. We also compute the proper charges and electric field components from Table 4-1. These values also relate to persistency. The persistency equations are determined by the inertial and tidal behaviors, Table 4-1, which have been computed numerically in sections 5.6 and 5.7. We start by checking that our solution meets the known conditions, section 5.5.

5.8.1 Electric field components $f^j{}_{o\upsilon}$

In Eq. (5.37), we argued that the *game value* sets the size of the charge gradient. More precisely, the *game value* sets the size of the electric field components $f^j{}_{o\upsilon}$, Eq. (5.35). We check that the electric field components (3.74) in the co-moving frame, Figure 5-16, match their initial values:

$$f^j{}_{o\upsilon} = \{0.4243 \quad -0.4243 \quad 0.1882 \quad 0.1882 \quad 0.2662\} \tag{5.56}$$

The order and color code is that blue, red, green, yellow and purple represent j in the directions $\{\xi_1 \quad \xi_2 \quad s_1 \quad s_2 \quad r\}$. The curves for green and yellow are on top of each other. The electric field determines the charge gradients $\omega_{\upsilon\alpha}$.

5.8.2 Proper charge components e_α

We call $\omega_{\upsilon\alpha}$ ***charge gradients*** since from Table 4-1, Eq. (3.69), they determine the behaviors of the *proper charges* e_α, Figure 5-17. The *proper charges* determine the mixed metric attributes, Eq. (3.51) that determines the relationship $E_j{}^o = -e_\alpha E_j{}^\alpha$ between *persistency components*, Eq. (3.54). This relationship shows that the *proper charges* are persistency attributes and demonstrates that the initial values of the *proper charge* are set by the initial values of the orthonormal set. Our choice of zero flow for the two prisoner directions translates to their corresponding *proper charges* being zero at the origin. The other proper charges are not zero, as seen in Figure 5-17. The proper charges also contribute to the active metric, Eq. (3.72), which we deal with in section 5.9.

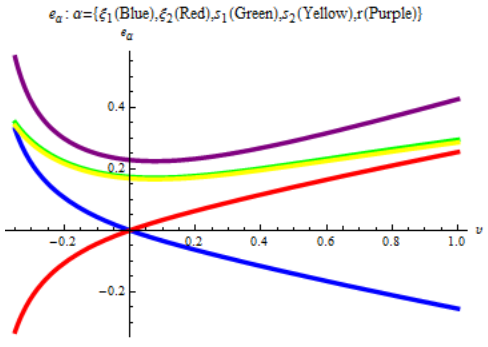

Figure 5-17: Proper charges $e_\alpha(\upsilon)$ in the co-moving frame

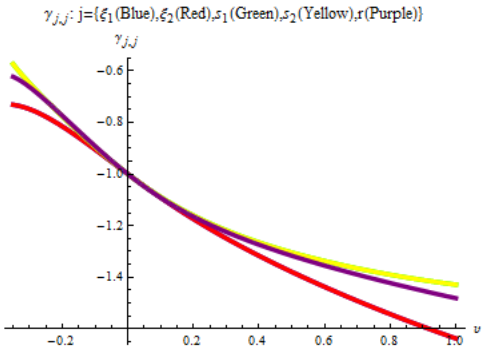

Figure 5-18: The components $\gamma_{jj}(\upsilon)$ in the normal-form frame

5.8.3 Inactive metric components γ_{jk}

In sub-section 5.7.1 we showed that the *bond compression volume* decreased as the active strategy υ becomes negative in the *co-moving frame*. We can show that this is also true in the *normal-form coordinate basis* by looking at the behavior of the diagonal components of the inactive metric components γ_{jj} using Eq. (5.55), Figure 5-18. As before, the color code is that blue, red, green, yellow and purple represent j in the directions $\{\xi_1 \quad \xi_2 \quad s_1 \quad s_2 \quad r\}$, respectively. We see that the diagonal components are all tending towards zero as we move left into the region that prisoner 1 becomes more engaged. The initial conditions were set assuming that the *co-moving frame* and *normal-form frame* were aligned at the origin.

The gradient of the metric potential determines the off-diagonal initial values of the *bond strain*, Eq. (5.38) in terms of the known payoff values of the prisoner's dilemma:

$$\partial_\upsilon \gamma_{jk}(0) = \left(\begin{array}{ccc|cc} -0.9466 & 0 & & -0.1414 & 1.2728 & -1.0000 \\ 0 & -0.9466 & & -1.2728 & 0.1414 & 1.0000 \\ \hline -0.1414 & -1.2728 & & -0.9762 & 0 & 0 \\ 1.2728 & 0.1414 & & 0 & -0.9762 & 0 \\ -1.0000 & 1.0000 & & 0 & 0 & -1.0057 \end{array}\right) \tag{5.57}$$

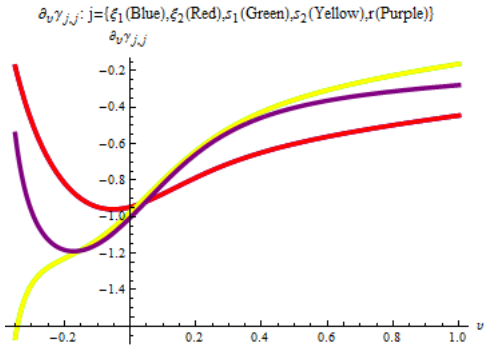

Figure 5-19: The components $\partial_\upsilon \gamma_{jj}(\upsilon)$ in the normal-form frame

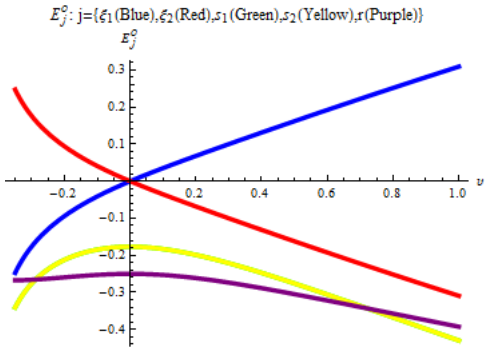

Figure 5-20: The flow components of the Killing vector $E_j{}^o(\upsilon)$

The initial off-diagonal gradient components are set by the payoffs Eq. (5.34), while the diagonal components are set by the compression coefficients Eq. (5.39) and show the shrinking of the space to the left compared to the right (Figure 5-19). The color code is the same as Figure 5-18. We suggest that with all other variables constant, a change along the utility for prisoner 1 represents a distance measure of $d\tau^2 = \gamma_{\xi 1 \xi 1} d\xi^1 d\xi^1$. Since the metric components go to zero on the left, we conclude that for two neighboring preferences at the origin compared to two neighboring preferences a distance to the left, there will be a perceived difference in distance as given by the connection components. These *persistency components* provide a mechanism for comparing utilities.

These results follow from a detailed quantitative analysis of the dynamic forces at play in decision making processes. In particular, they show that the payoffs, which determine the relative strategies players choose, vary as a function of the strategic value chosen. This mechanism is a key ingredient of *decision process theory*, one not found in *game theory*. The variation of the gradient of the metric (Figure 5-19) is clearly seen to produce a variation in the payoffs, Eq. (5.34). Despite these variations as a function of position, the metric potential gradients are *stationary* as a function of *proper time*.

5.8.4 Inactive flow components $E_j{}^o$

The behaviors of the metric potential are set by the *persistency components* Eq. (5.55). We gain further insight by looking in more detail at the behaviors of these *persistency components*. The flow components $V_j = E_j{}^o$ as seen in the *symmetric normal-form coordinate basis* are determined, Table 4-1, Eq. (3.64), by the acceleration and the charge gradients. Since we take the initial acceleration to be zero, the initial gradient is determined by the charge gradients. Because we start with charge gradients for the two prisoners that are non-zero, we obtain non-zero flows away from zero, Figure 5-20. The color code is that blue, red, green, yellow and purple represent j in the directions $\{\xi_1 \quad \xi_2 \quad s_1 \quad s_2 \quad r\}$, respectively.

The flow components can be interpreted as the coupling or charge with which the payoffs contribute to the streamline equations in the *symmetric normal-form coordinate basis*, Eq. (1.75). These flows correspond to conserved charges e_α. If we relax the condition in this model that there are *codes of conduct* strategies that are inactive, the corresponding flows will no longer be conserved. We get the important result that the players couple strongly away from the equilibrium point, which shows that *game theory* effects are strong away from such points. The charges for the two prisoners are opposite and equal for the model parameters chosen, though the equality is not significant since slightly changed initial conditions makes this equality disappear.

The flow for positive values of υ corresponds to player 2 being more ***aggressive***: this player is more engaged than the other based on the active variable u in Eq. (5.17). The model consequence is that player 2 demonstrates a ***greedy*** (negative) charge whereas player 1 demonstrates an ***accommodating*** (positive) charge. We view this result as important as *decision process theory* derives from *game theory* so we expect to see areas where *game theory* mechanisms are important.

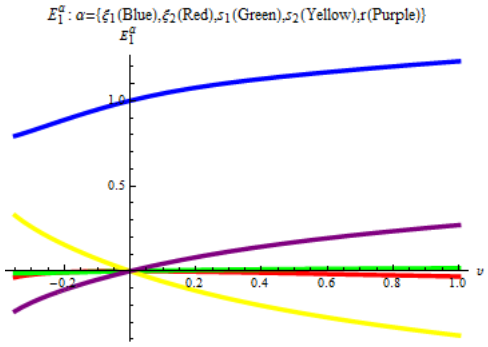

Figure 5-21: Prisoner 1 inactive Killing vector components $E_1{}^\alpha(\upsilon)$

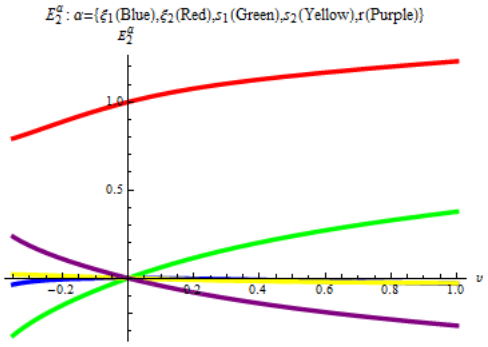

Figure 5-22: Prisoner 2 inactive Killing vector components $E_2{}^\alpha(\upsilon)$

5.8.5 Inactive transformation components $E_j{}^\alpha$

The spatial persistency components $E_j{}^\alpha$ that determine the transformation of the inactive strategies from the *symmetric normal-form coordinate basis* to the *symmetric co-moving basis* are determined by the compression and shear, Table 4-1, Eq. (3.67). We have already seen how the compression effect decreases the size of the *transformation cube* as we go to the left. Some evidence of this behavior is seen also in the components $E_1{}^\alpha$ for prisoner 1 in Figure 5-21, where the size of the proper direction for each player decreased in the *symmetric co-moving frame*. We have the color code blue, red, green, yellow and purple for the inactive directions α representing $\{\xi_1 \quad \xi_2 \quad s_1 \quad s_2 \quad r\}$, respectively. Similarly in Figure 5-22, we have the corresponding components for prisoner 2. In addition to the compression effects, the shear effects impose behaviors along the other directions.

5.8.6 Inactive determinant $|\gamma_{jk}|$

Certainly a main conclusion from our analysis is the striking configuration changes that depend on the active strategic value. This was exhibited in the co-moving frame by the behavior of the compression coefficient, Figure 5-10. Another measure of compression in the inactive space is the determinant of the inactive metric:

$$\gamma = \det \gamma_{jk} = |\gamma_{jk}| \tag{5.58}$$

This shows the same qualitative behavior, Figure 5-23. The invariant volume element is proportional to this determinant. Since this determinant goes to zero as we go left, it confirms that the yardsticks in the inactive space shrink in that direction.

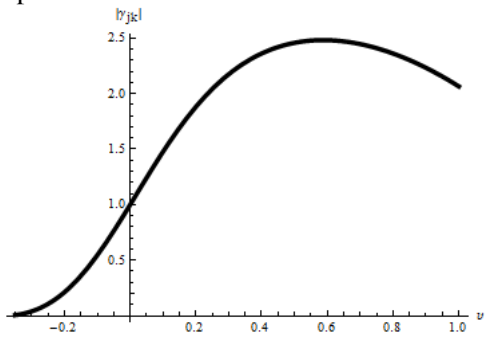

Figure 5-23: The determinant of the inactive metric $|\gamma_{jk}(\upsilon)|$

It also shows that the invariant volume shrinks if we go sufficiently far to the right. This is not so obvious from the behaviors that we have seen. A more detailed analysis shows that one of the eigenvalues of the metric is tending towards zero. Furthermore, the stresses are going to zero as we go far to the right.

In these last sections we have been concerned with the *stationary* behaviors that are a consequence of the *quasi-stationary hypothesis* of the *player fixed frame model*. We have identified the ingredients that determine behaviors as inertia, stress, strain and persistence. We next discuss the active behaviors that correspond to *proper time* and the *proper active relative player effort strategy*.

5.9 *Dynamic behaviors*

Even in the *stationary* view of the *quasi-static hypothesis* for the *player fixed frame model*, we have seen that inertial behaviors dominate the mechanism by which *structural stability* is maintained. The inertial stresses lead to the strains that we observe in decision processes as strategic flows, payoff fields and new effects not yet identified with the predicted strains. Furthermore, we have seen that the notion of distance in decision processes, which we tie intimately with the concept of measuring utility, is not an absolute concept, but a relative concept that depends on the frame of reference. In *rotating frames*, where the rate of strategic flow changes, distances can appear shorter as seen by an observer who is not rotating. The concept that distances are relative is a consequence of the covariant nature of our *decision process theory*. This disconnects the underlying topological space from the quantitative measures of nearness. This connection is broken for our measure of time differences as well. However to see such effects, we need to turn to the dynamic behaviors of the theory.

Not only are the flows dynamic in the sense that the *stationary* flows may exhibit accelerations, they are dynamic in the sense that they explicitly depend on time. In a gauge theory, measure of time intervals depends on the metric potential, Eq. (1.72). In this section we explore the dynamic behaviors that result from our *decision process theory* with numerical examples for the prisoner's dilemma. The metric potentials are determined by the flow and coordinate transformations, so we start with their behaviors based on the streamline solutions to Table 4-1 provided in section 4.6.

We have two results in common with the theory of relativity in physics: Our conception of time differences depends on frame and the metric potentials with which we analyze distances can form steady-state waves. In both cases we rely on the relationship between the active metric and the transformations, Eq. (3.72):

$$g^{ab} = \left(1 + e_\alpha e^\alpha\right) E^a{}_o E^b{}_o - E^a{}_\upsilon E^b{}_\upsilon \tag{5.59}$$

We observe that with the boundary conditions we have imposed for the prisoner's dilemma, the components of the metric are initially:

$$\begin{aligned} g^{tt} &= \left(1 + e_\alpha e^\alpha\right) \equiv \psi \\ g^{tu} &= 0 \\ g^{uu} &= -1 \end{aligned} \tag{5.60}$$

Distances in time result when we don't change the active strategy:

$$d\tau^2 = g_{tt} dt^2 \tag{5.61}$$

At our initial point (the origin), the metric $g_{tt} = \psi^{-1}$ is determined from the proper charges, Figure 5-17. Because of the initial payoffs, this is non-zero and has a minimum at the origin. The origin is where the inertia is greatest and where the acceleration is zero. We now see this is where we expect time to move most slowly.

In this section we show that in areas with large inertia, any quantitative measure of time slows down. Not all parts of the topology can be reached from a given starting point: boundaries are set by areas where the components of the metric field vanish. We show that steady-state wave solutions exist, exhibiting curvatures determined by these boundaries.

To carry out our calculations, we have to expand what we mean by known conditions, section 5.5. Normally we would specify the flows and payoffs for all strategic values at a *proper time* of zero. We borrow however an idea from engineering, which is to create solutions that provide insight given our expectations that such normal specifications could be built up from *harmonics* starting with *stationary* solutions, solutions linear in time and then solutions built from *harmonics* or *phasors*. In mathematics, such solutions provide a Fourier analysis from which to build any solution, including the one of interest where we know the initial conditions. For our purposes, *harmonics* as approximated by the *harmonic polynomials* Eq. (4.98) for the *streamline solutions* of section 4.6 fulfill our need. We have only to specify which *harmonic polynomials* we will focus on.

Unless stated otherwise, the illustrative results in this section are based on *harmonic polynomials* of degree $N = 50$. We consider *proper times* in the interval $[0,1]$ and consider solutions that are linear on which there is a single *harmonic* added of frequency $\varpi = 10$. For these solutions, we are not looking for an engineering solution to a particular problem. Rather we hope to survey the types of behaviors expected. We are free therefore to pick nominal values for the *harmonic polynomials*:

$$\begin{aligned} x^t &= a^t + b^t \tau - \frac{0.05}{\varpi} \sin_N \varpi\tau \\ \partial_\upsilon x^t &= a^t \\ x^u &= a^u + b^u \tau - \frac{0.2}{\varpi} \cos_N \varpi\tau \\ \partial_\upsilon x^t &= a^t \end{aligned} \tag{5.62}$$

These equations determine the behaviors away from the origin $\upsilon = 0$ of zero *proper relative player effort*. The linear terms are determined by ordinary differential equations whose initial conditions are set by the flow boundary conditions and the Gramm-Schmidt orthogonalization process described in section 5.5. Obviously many other choices other than Eq. (5.62) are possible, some of which will be discussed in section 5.10 where we do a sensitivity analysis of our results.

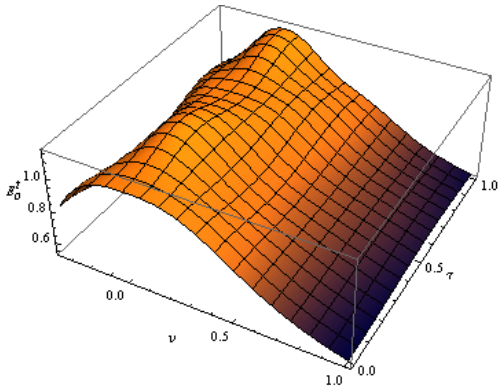

Figure 5-24: The *flow* along time, $E^t{}_o(\upsilon,\tau)$

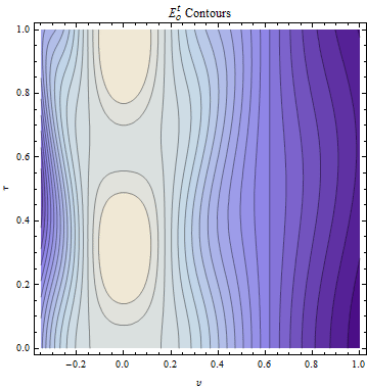

Figure 5-25: The contour plot for the *flow* along time, $E^t{}_o(\upsilon,\tau)$

As a recap, the symmetric prisoner's dilemma is formulated as a *player fixed frame model* using the *quasi-stationary hypothesis*. It is a *single strategy model*, whose *streamline solutions* and required scalar equations are detailed in section 4.6. We have considered the inertial behaviors Table 4-6 in section 5.6, the electromagnetic and tidal behaviors Table 4-4 and Table 4-5 that generate strain in section 5.7 and the persistent behaviors of Table 4-1 in section 5.8. In this section we use Table 4-1 to provide the dynamic behaviors of the flows $E^a{}_o$ and the transformations $E^a{}_\upsilon$ to the proper active direction that depend on the *proper time*. The partial differential equations that result are Eq. (4.112), whose solutions in terms of *harmonic polynomials* can be obtained from Eq. (4.144). The major result of this section is to show that these equations are effective tools to provide the time dependence of the theory. We are not currently aware that these techniques have been used elsewhere.

5.9.1 Dynamic flows $E^a{}_o$

We start by looking at the flow component for time as a function of both strategic direction υ and *proper time* τ, Figure 5-24. We see two effects: first the general shape results from the linear terms. Without the *harmonic polynomial* contribution the flow would be independent of time. The strategic dependence is a consequence of the inertia and is distinct from the effects of the proper charge. The second effect is due to the single *harmonic* contribution that we have added to the holonomic time scalar x^t. From the *harmonic* disturbance generated in time, a *harmonic* disturbance is also generated in space.

We see the effects of the *harmonic polynomial* contribution more clearly in a contour plot for the time flow, Figure 5-25. In this contour plot, we see two peaks along the origin; away from the origin we see a small peak to the right. There is the start of a steady-state travelling wave that moves from the left to the right.

To get a complete picture for the time component of the metric we need the component of flow along the active direction, which we take to be initially zero. Though for a linear solution the flow would remain zero, the *harmonic polynomial* contribution provides a non-zero oscillation for the flow, Figure 5-26. We see that the flow indeed starts at zero. The initial behavior set by the *harmonic* $\cos_N \varpi\tau$ for the distance behaves like $\sin_N \varpi\tau$ for the flow and thus starts at zero. Along the streamline from the origin, this *harmonic* behavior generates spatial oscillations that are clearly displayed based on our initial conditions. We see more clear evidence of the travelling waves.

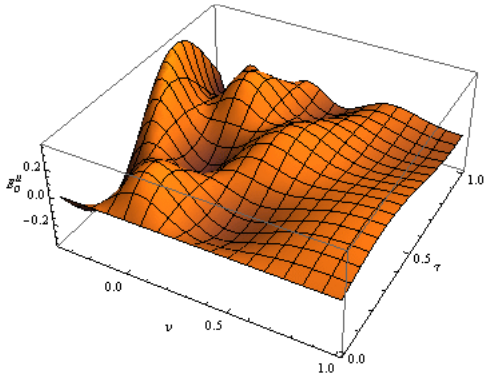

Figure 5-26: The *flow* along the active strategy $E^{u}{}_{o}(\upsilon,\tau)$

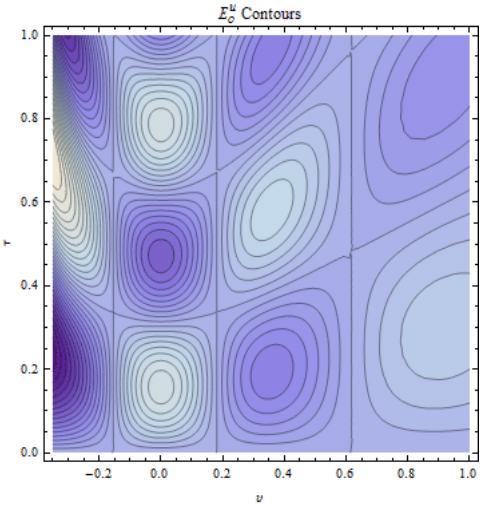

Figure 5-27: The contour plot for the *flow* along the active strategy $E^{u}{}_{o}(\upsilon,\tau)$

The travelling wave behaviors are clearly visible in the contour plot, Figure 5-27. Here we see the distortions that reflect the difference between our wave equation, Eq. (4.112) and the usual wave equation. We see that the null lines between the peaks and troughs are not at right angles. Furthermore they bend at the boundaries at the left, determined by the vanishing of the inactive metric components. The direction of the travelling wave also bends due to the same boundary. If we think of the peaks as being places where inertia collects, then the motion of the inertial peak is the movement of energy density. This motion should be less than the maximum speed possible and should form an angle of greater than 45 degrees.

5.9.2 Active metric components g^{ab}

We have the main components of the metric g_{tt}, which is formed from the inverse of the metric components g^{ab}. The result, Figure 5-28, shows the inertial effect and proper charge effects, which are both static. On top of these two static effects is a ripple in the measurement of time due to the *harmonic polynomial*. Because of the ripple, there will be local minima in which inertia can be trapped.

We see structure that is in addition to the big picture behavior of the trapping field formed from the stress and proper charges. Not only is our notion of time influenced by the acceleration frame, so is our notion of distances along the strategic direction, Figure 5-29, where the main components come from the transformation $E^{u}{}_{\upsilon}$, Figure 5-30 and a somewhat smaller contribution from $E^{t}{}_{\upsilon}$ not shown. As with the time flow, there is a static behavior on which there is a small ripple effect due to the *harmonic polynomial* contribution. It is significant that the wave equation properties one sees in physics are reflected here as well. *Harmonic* behavior in time leads to *harmonic* behavior in strategy space; *harmonic* behavior in space leads to *harmonic* behavior in time. Because the equations, though more complicated than the usual wave equations, are still linear we conclude that a localized event at an initial point in time and space will radiate outwards in both time and space.

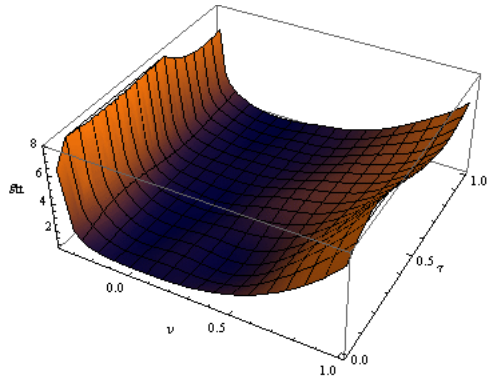

Figure 5-28: The metric potential $g_{tt}(\upsilon,\tau)$

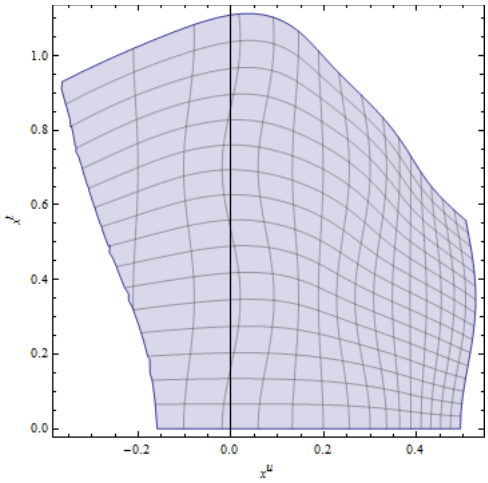

Figure 5-29: distance $x^u(\upsilon,\tau)$ **versus time** $x^t(\upsilon,\tau)$ **for constant** (υ,τ) **contours**

In Figure 5-29, the horizontal curves represent constant values of *proper time*, while the vertical curves represent constant strategic values of *proper relative player effort*, which we call ***streamlines***. If we think of the curves of constant *proper time* as representing events with the same "age", we conclude that aging appears differently in the *symmetric normal-form coordinate basis* depending on the initial *proper relative player effort*, which follows from the dependence of the gradient of *proper time* with acceleration, Eq. (4.129), exercise 24 section 4.8. Roughly we can say that a decision process that occurs in an area of high energy density takes longer than the same process in an area of low energy density.

The net effects can be computed for g_{uu}, Figure 5-31. There are boundaries of the space on the left and ripples on the right that propagate outward in time.

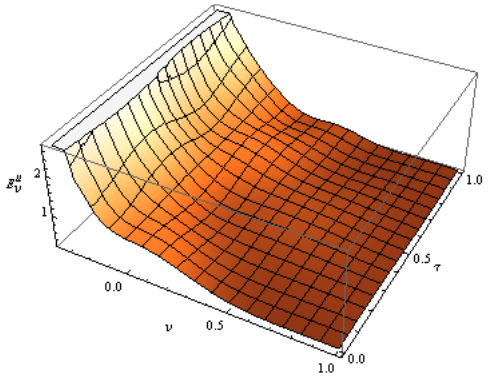

Figure 5-30: The transformation of the active component $E^u{}_\upsilon(\upsilon,\tau)$

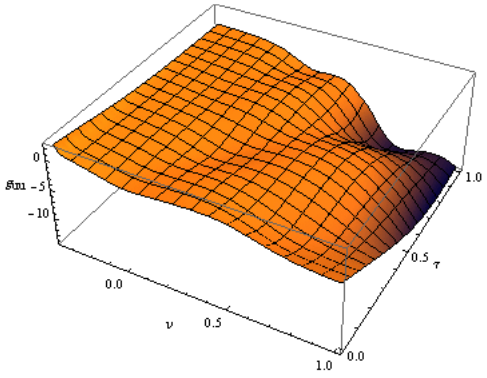

Figure 5-31: The metric potential $g_{uu}(\upsilon,\tau)$

There are two general characteristics we glean from these calculations. First, we require a ***causality principle***: signals between two points can't go faster than a null-geodesic (exercise 11): $g^{tt}>0$. We see evidence that we approach this boundary when surfaces of constant *proper time* start to bunch together. Causality for decision processes is the common sense view that future events can't be influenced by past events instantaneously: a sufficient time must pass for the future event to become aware of the past action. In *decision process theory*, the mechanism for communication stems from the wave function and the fact that there is finite maximum speed for signals to propagate. Such propagation effects will be observed

both in the metric potential fields as well as the payoff fields. They are analogous to gravitational waves and electromagnetic waves respectively.

Secondly, we require the seemingly obvious ***principle of possible change*** at any point in space time, change is always possible. In other words, strategies can change in time. What makes this not so obvious is that strategies can't change faster in time than a signal along the null geodesic. If the velocity along that null geodesic goes to zero, change becomes impossible. This occurs whenever streamlines begin to bunch together. We see evidence of this in Figure 5-29. As we get more bunching, we require g_{uu} to become large or correspondingly g^{uu} to approach zero, Eq. (5.73). We must have $g^{uu} < 0$ as a requirement to enforce the principle of change (exercise 12).

With these example behaviors using just a single *harmonic polynomial* contribution, we see dramatic changes in the character of the *stationary* solutions. We go from a solution with a single potential well to solutions with multiple wells. We might well think of this as analogous to galaxy formation. These additional pockets of *structural stability* are consequence of a single frequency dominating. To prove that this is so would be to investigate in more detail the initial spatial distributions. It is not difficult to argue however that a pulse of events localized in time might be similar to a pulse located initially in space. Such a pulse would correspond to a number of frequencies around some common average frequency. In other words, we would argue that a single frequency might occur corresponding to a localized energy density distribution. Our figures are not too dissimilar to that set of assumptions.

5.10 *Sensitivity Analysis for dynamic behaviors*

We have provided an engineering view of the large scale structure of the solutions, not unlike the view taken by (Hawking & Ellis, 1973) of Einstein's general theory of relativity. This provides insights quite different from those obtained using weak field approximations to these theories. Therefore, despite the simplicity of the model for the prisoner's dilemma and the relative simplicity of the ***common good solution***, we obtain non-simple structures in variations around this base. As part of our sensitivity analysis of *stationary* solutions in section 5.6, we introduced an alternative ***Nash solution***, which illustrates additional characteristics. The major difference between the *common good* and *Nash* solutions was set by the initial strategies. We discussed the effect of setting the expected *game value* to zero in each case.

In this section we investigate the sensitivity based on time dependent dynamic behaviors. To articulate the major possibilities, it will be sufficient to consider only the *Nash* solutions with a small initial pressure $p = 0.01$ and zero *game value*. By using a small initial pressure and zero *game value*, we suppress the effects we have already studied in section 5.6 that generate charge gradients. We use the *harmonic* parameter values used in section 5.9. They provide a baseline that facilitates our understanding of the effects.

Table 5-1: Player stakes and decision beta choices for sensitivity analysis

	Low β	Baseline β	High β
Low stakes	$\{\sigma = 1/10,\ \ \beta = 1/10\}$	$\{\sigma = 1/10,\ \ \beta = 1/3\}$	$\{\sigma = 1/10,\ \ \beta = 9/10\}$
Baseline stakes	$\{\sigma = 1,\ \ \beta = 1/10\}$	$\{\sigma = 1,\ \ \beta = 1/3\}$	$\{\sigma = 1,\ \ \beta = 9/10\}$
High stakes	$\{\sigma = 10,\ \ \beta = 1/10\}$	$\{\sigma = 10,\ \ \beta = 1/3\}$	$\{\sigma = 10,\ \ \beta = 9/10\}$

We consider different values for the game beta β and (equal) player stakes $\sigma_1 = \sigma_2 = \sigma$, which we choose from Table 5-1. These choices have a major impact on the time component g_{tt} of the metric that determines the behavior of time intervals, Eq. (5.61). In a qualitative way we anticipate the effects from the numerical calculations by taking the first term of Eq. (5.59):

$$g_{tt} \approx \left(1 + e_\alpha e^\alpha\right)^{-1} \left(E^t{}_o\right)^{-2} \tag{5.63}$$

The first factor is determined by the proper charges, Table 4-1. We recall from our previous numerical results, Figure 5-17, that the initial proper charges are set by the initial flow; for those values of flow that are zero, the corresponding proper charges are zero. Thus we expect the first factor to be governed by β. The second factor initially depends on the strains (since we have chosen the stresses to be very small). In particular the payoffs determine the (reduced) shear, Eq. (5.53). If we increase or decrease the payoffs by an order of magnitude, we expect these shear values to vary proportionately.

5.10.1 Baseline

So our rough expectation is that β, an attribute of the inertial field, governs the first factor and σ, an attribute of the payoff field, also governs the second factor. The second factor gives rise to the *harmonic* behaviors. We start by examining the baseline form for the metric contour, Figure 5-32, for the Nash solution with small pressure $p = 0.01$ and zero *game value*. The ***focus area*** for the decision process, the allowed space of strategy values υ, is bounded below at approximately $\upsilon = -0.58\ldots$. Much below this the equations become singular. We can go much higher that $\upsilon = 1$, though it requires progressively more *harmonic polynomial* terms to get reliable results. We obtain a lattice picture that is truncated by the *focus area*. As in our previous dynamic calculations, we see the effects of our modified wave equation.

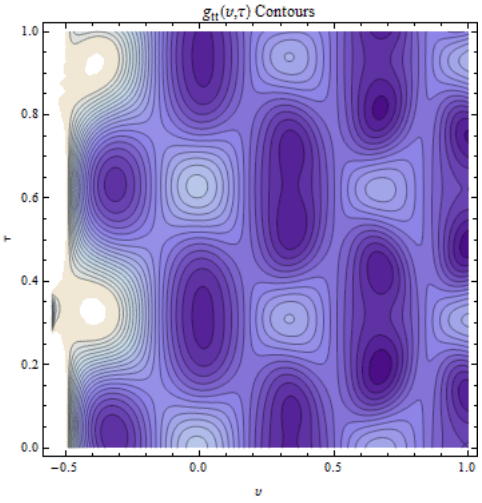

Figure 5-32: Baseline contour plot for $g_{tt}(\upsilon,\tau)$

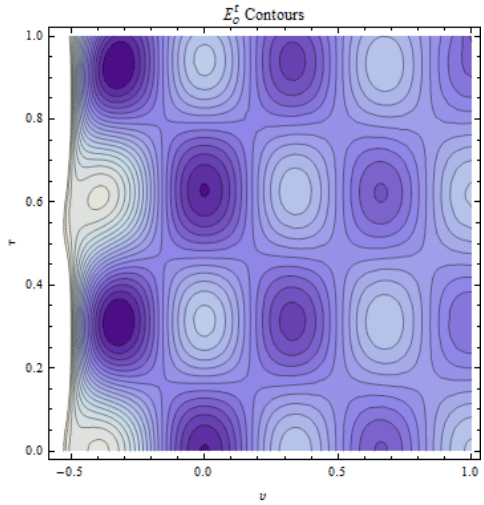

Figure 5-33: Baseline contour plot for the *flow* $E^t{}_o(\upsilon,\tau)$

The baseline contour plot for the flow $E^t{}_o$, Figure 5-33, displays an even more distinct lattice structure without the focus contribution from the proper charges. The lattice structure is by no means an obvious consequence of the partial differential equations Eq. (4.105). The result is a consequence of the acceleration being small so that the terms in the partial differential equation that depend explicitly on *proper time* can be ignored. This is not exact nor is the lattice dependence uniform.

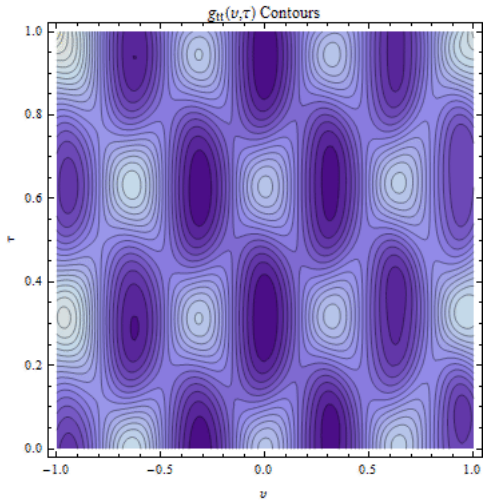

Figure 5-34: Low stakes and low β contour plot for the metric $g_{tt}(\upsilon,\tau)$

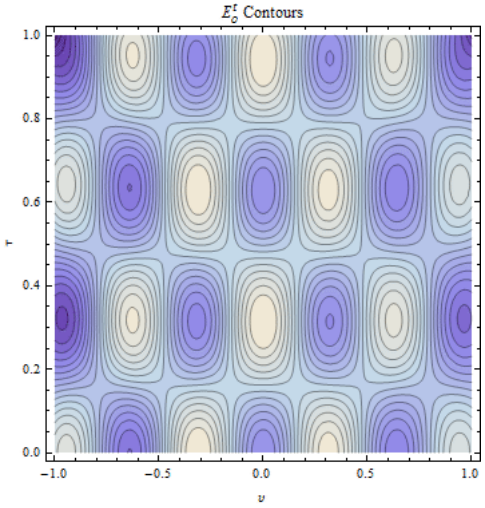

Figure 5-35: Low stakes and low β contour plot for the *flow* $E^t{}_o(\upsilon,\tau)$

5.10.2 Low stakes, high stakes

To widen the *focus area*, we go to the case with low stakes and low β, where we expect little contributions from the strain, little contributions from the proper charges (based on small β) and large contributions from the *harmonic* contribution. We get the expected result that the charge gradients are almost zero, the proper charges are small and the first factor in Eq. (5.63) is almost unity. The potential well comes almost entirely from the *harmonic* contribution; there is a negligible contribution from the initial shape of $E^t{}_o(\upsilon,0)$. This is clearly displayed in the contour plot, Figure 5-34. The *focus area* for the decision process is expanded from the baseline case.

The contour plot shows lines of $\beta=\pm1$, such as the two that start at the origin. The light color indicates peaks and the dark color indicates valleys. For this case we replicate the *harmonic* wave equation and phasor solutions. The underlying lattice structure is seen more clearly in the flow $E^t{}_o$, Figure 5-35. We see a hexagonal packing pattern. The light color areas indicate the path taken along the minimum of the potential, since the inverse square of the flow is approximately the metric component.

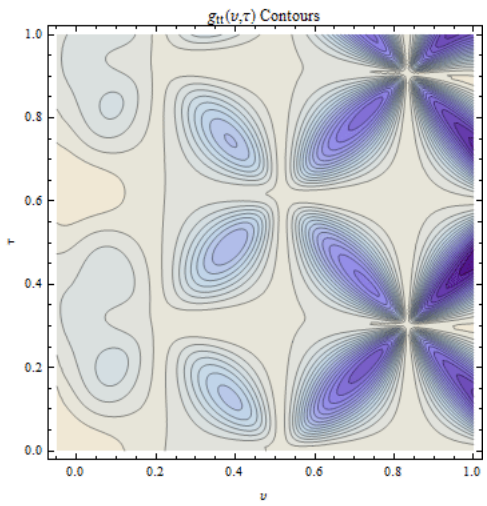

Figure 5-36: High stakes and low β contour plot of $g_{tt}(\upsilon,\tau)$

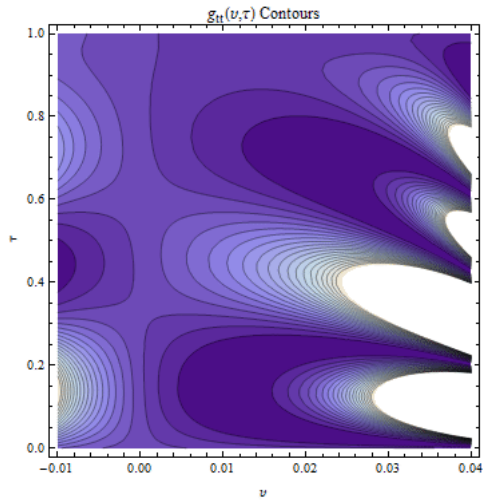

Figure 5-37: High stakes and high β contour plot of $g_{tt}(\upsilon,\tau)$

An alternative but not equivalent way to narrow the *focus area* is to consider high stakes and low β. In this case we modify the shear components, which influence the time structure, the lattice pattern and narrow the *focus area*, Figure 5-36. As we move away from the origin along the strategic axis, there are progressively deeper potential well pockets, indicating a degree of instability. The energy generating these pockets comes from the payoffs and the assumption of high stakes. The higher stakes along with *harmonics* generates the effect. If we remove the *harmonic* contribution we don't expect the same structure. The striking feature of the contour plot is the clover leaf pattern, an unexpected consequence of the partial differential equation. The clover leaf pattern is not distinct in the contour for ${E^t}_o$.

The final case we consider is high stakes and high β, which has solutions for only a narrow range of the proper distance, approximately $\upsilon \in [-0.02, 0.05]$, Figure 5-37. Note that if we changed the solution to one in which the initial flow has each player confessing, $V^a = \{0 \quad 1 \quad 0 \quad 1 \quad m\}$, then we would also obtain a clover leaf pattern such as Figure 5-36. For high stakes and high β, the *focus area* is smaller and structure is less distinct. For this case, there is even indication that space-time becomes disjoint.

These are significant consequences and they are based on the size of the payoffs. They are in addition to the effects based on the relative values and the benefit to the players on the expected *game values*. In addition to the inertia effects associated with the energy density and pressure, there are consequences based on the β characteristic or speed of the flow, which is also a type of inertia. One reflects a tendency each player may have to favor certain strategies. This we associate with the energy density and pressure. A high inertia suggests that the players are reluctant to change their style of play. However, we might consider a version of chess in which there is a timer. This changes the speed at which the game is played. A very high speed version of chess would be a high stakes game, which introduces a very different aspect of the inertial fields.

We speculate that the latter definition of inertia is significant in physical theories of cosmology. Early eras of the universe might be characterized primarily as radiation, so that this would correspond to a high β era. Things don't clump together. In contrast, the current era would be a low β era. Galaxies have formed; there is a lot of clumping. These characteristics hold in decision processes. At very high speeds, clumping does not occur (compare Figure 5-36, clumping with Figure 5-37, and no clumping). Thus we believe the effects we have identified in this section are essential. Both the speed β and stakes σ play a role that has not been accounted for in the standard game theory approaches. They determine the *focus area* and structure of the decision process.

In this and the last section, we have provided the time dependent dynamic behaviors we expect for the prisoner's dilemma in the *co-moving coordinate basis*. In the next section we return to the original *normal-form coordinate basis* and examine the dynamic behaviors we expect for the payoffs.

5.11 *Normal-form behaviors*

There are many ways of investigating the dynamic behaviors in our *decision process theory*. If we are given the behaviors of the system at an initial point in time for all possible active strategy values, we can then compute the behavior of the system as a function of *proper time*. We equally well gain insight into the system by considering the behavior of the system as known at a single strategic point and all times, which for us is the presumed equilibrium point $\upsilon = 0$. The behavior of the system is predicted by the equations for all other strategic values υ. The latter approach leads to the former approach by superposing the *harmonic* solutions to achieve any given strategic behavior υ of the system at initial *proper time* $\tau = 0$. This approach corresponds in concept to the phasor analysis of circuits in electrical engineering. Examining the response of a stable system to a known perturbation is also common in system dynamics, for example, (Senge, 1990).

Recall from section 5.5 that initially, the flow represents the strategy choice of each prisoner, Figure 5-38. One possibility is that this flow is constant. We explore dynamic possibilities by superposing a *harmonic* onto this constant behavior. The color code is that blue, red, green, yellow and purple represent the directions $\{N_2 \quad C_2 \quad N_1 \quad C_1 \quad t\}$. We clearly see the assumption that each player starts with the strategy to not confess (blue and green), with no strategy to confess (red and yellow). The time strategy (purple) reflects the baseline value for $\beta = 1/3$. We see the *code of conduct* imposed that the flow to confess is zero and so these flows oscillate around zero.

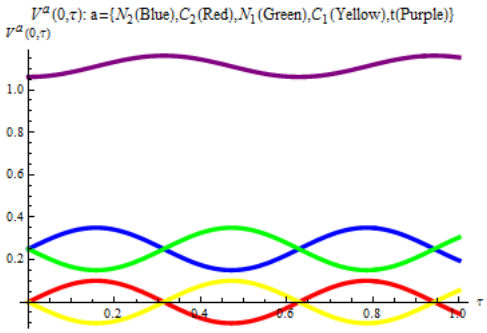

Figure 5-38: The flows for the prisoner's dilemma in the original normal-form frame

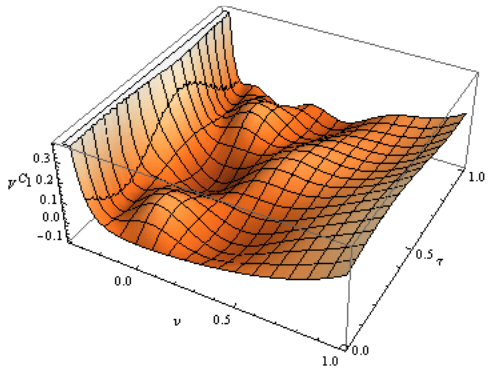

Figure 5-39: The flow for prisoner 1's choice to confess as a function of (υ, τ)

The *harmonic* disturbance propagates outward in space, Figure 5-39. In this case we see that the *focus area* narrows causing the effects of the *harmonics* to damp out. Furthermore we see that at both extremes, the prisoner chooses some amount of the confess strategy. We expect to see these effects in the payoffs and other strain parameters. It will be more insightful if we consider the transformed version of the space, Eq. (5.16), with Eq. (5.17) for the behaviors that are internal to the *decision process theory*.

In this basis we have the payoff field contributions $F^j{}_{tu}$, which can be determined from the co-moving frame field $f^j{}_{ov}$, Table 4-1, Eq. (3.30):

$$F^j{}_{tu} = \frac{f^j{}_{ov}}{E^t{}_o E^u{}_\upsilon - E^u{}_o E^t{}_\upsilon} \tag{5.64}$$

As expected, the *stationary* behavior of the numerator for the prisoner's dilemma model parameters, Figure 5-16, is modified by the time dependence of the denominator. The behavior has by assumption the

single *harmonic* time dependence at $\upsilon = 0$, Figure 5-40. We see the *harmonic* wave in the figure for the electric field components. The color code is that blue, red, green, yellow and purple represent j in the directions $\{\xi_1 \quad \xi_2 \quad s_1 \quad s_2 \quad r\}$. Notice that the electric field exhibits a travelling wave behavior. We explore such behaviors further in the next chapter.

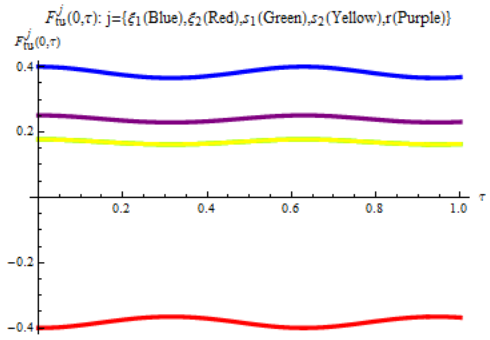

Figure 5-40: Electric field $F^{j}{}_{tu}(0,\tau)$ in the normal-form coordinate basis

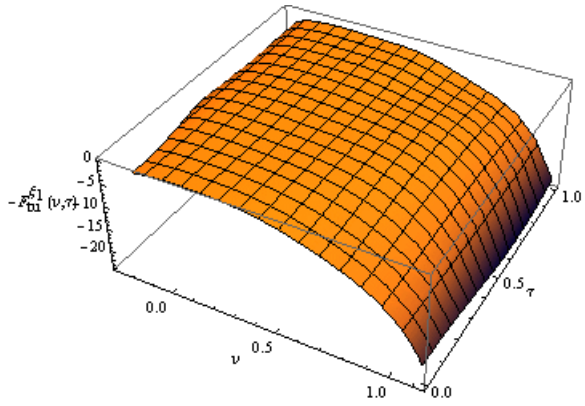

Figure 5-41: Electric field $-F^{\xi_1}{}_{tu}(\upsilon,\tau)$ in the normal-form coordinate basis

The rather small *harmonic* in ξ_1 for example is seen to be damped out quickly. Most of the behavior of this electric field component is set by the restriction in size of the *focus area*. As we saw in section 5.10 with the sensitivity analysis, higher stakes and a lower β along with a lower initial pressure at the origin all contribute to making the results more sensitive to the *harmonic*.

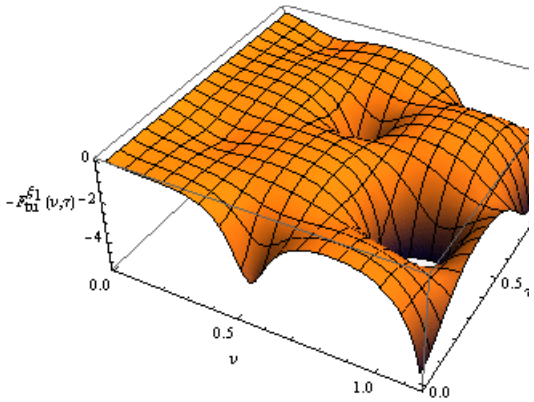

Figure 5-42: High stakes low beta version of the electric field $-F^{\xi_1}{}_{tu}(\upsilon,\tau)$

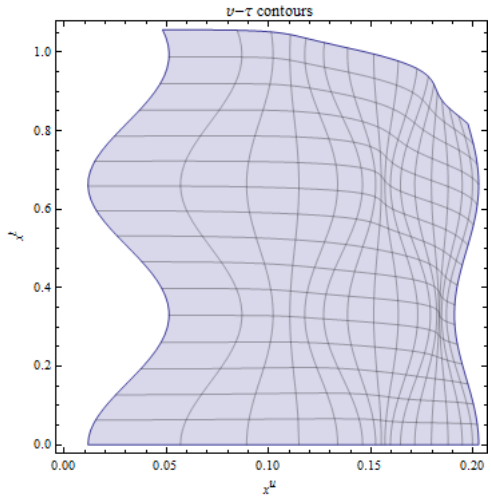

Figure 5-43: distance $x^u(\upsilon,\tau)$ versus time $x^t(\upsilon,\tau)$ for constant (υ,τ) streamlines

If we use the same analysis as section 5.10, Table 5-1, for high stakes and low beta, we get a vastly different structure for the electric field component for ξ_1, Figure 5-42. In both this and the previous figure we start with the same presumption of the time dependence as being *stationary* with a small *harmonic*. With high stakes and low β, the system resonates or "rings" more dramatically and over longer (proper)

distances than in the former case. However, the physical size of the system is smaller, Figure 5-43. In some sense the system is more ***brittle*** when the stakes are high.

Since the *electric field* components reflect and replace the concept of *game value* or expected payoffs, the brittleness reflects the risk inherent in such high stakes decision processes.

5.12 *Outcomes*

The student will have learned that the prisoner's dilemma demonstrates that a player *code of conduct* can be imposed in *decision process theory* and such hypothesis leads to a "stable" set of solutions. The theory thus extends the notion of solutions based on Nash equilibrium in *game theory*, which provide another class of "stable" solutions. By adding a *code of conduct* to the prisoner's dilemma, the *player fixed frame model* for the prisoner's behaviors reduces to a single active strategy. Complete numerical solutions to these models are obtained that represent both stationary and non-stationary dynamic behaviors.

The dynamical behaviors reflect both a topological ordering of time and strategic events that is common to game theory formulations as well as a measurement or ***gauge structure*** within this topology that provides a fabric on which decision events occur. The fabric construct, or connection, has both energy and momentum and influences and can be influenced by decision processes. The student will see from the numerical calculations, analytic evidence for inertial mechanisms associated with the stresses on the fabric and the speed β of the energy flow. Non game-theoretic results are obtained such as evidence for effects due to the *stakes* of the process as well as to the expected *game value*.

Because systems that balance forces share energy from one part of the system to another, the student is led to the view that energy is the key transferable quantity that replaces the classical notion of *game value* (see the ***law of opportunity***, section 7.7). All physical systems can transfer energy; the student will note that one form of that energy is the subject's potential energy per unit charge and that in the prisoner's dilemma model, it is closely related to the prisoner's expected *game value* payoff. These inertial and payoff mechanisms are new and specific to the gauge theory framework adopted.

By studying the numerical models, the student learns that the results are based on a causal evolution of behavior starting from an initial surface at zero *proper time* or equivalently, an initial surface at zero strategic distance (from a presumed equilibrium for example). This demonstrates that payoffs are functions of strategies that are in general different away from that initial surface. The allowed ranges are determined by the *causality principle* and the *principle of possible change*.

In this chapter, the student will have learned a behaviorist (rather than a psychological) view of the prisoner's dilemma and a formulation of this view inside a dynamic theory. The view was limited to the *player fixed frame model* and a single active strategy, which served to show that applying a *code of conduct* leads to stable solutions. The student should also appreciate that with the *quasi-stationary hypothesis* of section 4.5, all strategies can be active. The methods for solving these equations may require different numerical techniques (Courant & Hilbert, 1962). Mechanical and electrical engineering disciplines solve problems of a similar nature (Bhatti, 2005) and their techniques may be applied to the partial differential equations Eq. (4.94). Multiple active strategies introduce new attributes a^{υ} from the commutation rules Eq. (4.75). Nevertheless, the same techniques of analyzing the solutions in terms of *harmonic polynomials*, Eq. (4.98) is possible using *Mathematica*© and the ***numerical method of lines***, (Wolfram, 1992).

The attainment of the outcomes of this chapter is facilitated by doing the exercises in the following section. Based on this investment, the student should achieve the more detailed outcomes below based on section.

- In section 5.1, the student will have learned the relevance of altruism and egotism from (Thomas & Kane, 2008), where it is suggested that empirical investigations of human participants presented with prisoner-dilemma game situations have yielded interesting results that contradict standard game theory analysis (see (Sally, 1995) for a review). Some of these results have motivated so-called "psychological" game theories (e.g., (Dufwenberg &

Kirchsteiger, 1998); (Rabin, 1993)). The hallmark of these psychological frameworks is that they attempt to model players' "fairness" or "kindness," as well as each player's *beliefs* about whether his or her own actions will be reciprocated with (un)kind or (un)fair actions. As (Rabin, 1993, p. 1281) notes in his psychological model, the notion of *altruism* can bear on the notion of fairness: "*the same people who are altruistic to other altruistic people are also motivated to hurt those who hurt them"* (emphasis in original).

- In section 5.2, the student recalls the normal form of the prisoner's dilemma.
- This is followed in section 5.3 with ways of writing the payoffs and strategy vectors that are equivalent in *game theory* but whose consequences may be dynamically different in *decision process theory*.
- The concept of the *code of conduct* is introduced in section 5.4. By identifying certain active strategies as dynamically inactive, an internal symmetry is introduced that is stable in the sense that small changes away from that choice lead to small changes in behaviors. This is a general property of the hyperbolic partial differential equations of the theory.
- Hyperbolic partial differential equations have stable solutions given an appropriate specification of scalars on a hyperplane transverse to a time-like vector. The flow provides the time-like vector and the hyperplane is a surface transverse to the flow. The appropriate scalars are the transformations from the *symmetric normal-form coordinate basis* to the *symmetric co-moving coordinate basis*. The student will be able to set these appropriate values based on section 5.5: the student will be able to specify the known flows, set the values for the orientation potentials for the symmetric prisoner's dilemma, transform these values from the *symmetric normal-form coordinate basis* to the *symmetric co-moving orthonormal coordinate basis* and deal with the specification of inertial.
- From section 5.6, the student will be able to determine when inertial effects are needed to support a *code of conduct* or non-zero *game values*. To obtain a solution of the prisoner's dilemma that supports the *common good* of the prisoners, one must have inertial or stress effects to overcome centrifugal effects due to the charge gradients $\omega_{\upsilon\alpha}$. To obtain *fair* solutions that are based on self-interest and reflect the Nash equilibrium, no such inertial effects are needed.
- From section 5.7, the student will learn the importance of the strains that are the results of the inertial stresses. In the *quasi-stationary hypothesis*, the strains are *stationary* and are determined from the known conditions. Compression components and charge gradients result from payoffs and equilibrium strategies that are not Nash equilibriums. Such components generate inertial attractive effects similar to gravity as well as repulsive effects due to pressure gradients. Shear effects are present as well, which in the symmetric prisoner's dilemma are attributes of the initial payoffs.
- From section 5.8, the student will be able to trace the effects of the stresses and strains in the theory to the persistency components $\left\{E_j{}^o \quad E_j{}^\alpha \quad E_j{}^\upsilon\right\}$. The student will understand the mechanism that generates the important new effect in *decision process theory* that payoff values change as a function of strategy. The student will also understand the mechanism for charge or coupling that determines the size of *game theory* effects in the theory. A result that has possibly wider applicability is that an *aggressive* player displays a *greedy* charge whereas the other player has an *accommodating* charge.
- From section 5.9, the student learns from a simple example that *harmonics*, approximated by *harmonic polynomials* generate substantially new behaviors that require two principles: causality and change. The behaviors also demonstrate that in *decision process theory*, the measurement of time is relative to the frame of reference as is the measurement of space. Dynamic behavior exhibits two related principles: the *principle of causality* and the *principle of possible change*. Both refer to the characteristic of *decision process theory* that the

mechanism of communication is by sending signals that must travel at a non-zero but finite speed, which is set by the transmission speed of the wave equations.

- In section 5.10, from a sensitivity analysis the student learns that there are significant dynamic effects related to the *stakes* associated with a decision. Qualitative new behavior are exhibited when the *stakes* are sufficiently high. This is in marked contrast to *game theory* where the stakes have no strategic effect.
- In section 5.11 the student learns the behaviors expected for the prisoner's dilemma in the original *normal-form coordinate basis*. The code of conduct imposed on the solution is now clearly visible. The student learns that the concept of *game values* are effectively replaced in *decision process theory* by the *electric field payoff values*.

5.13 *Exercises*

1. Show that the transformation S converts the coordinates in the seven dimensions of time and space for the prisoner's dilemma to Eq. (5.16), where the order of the coordinates is $\{t,\ \xi_1,\ \xi_2,\ N_2,\ C_2,\ N_1,\ C_1\}$:

$$S = \begin{pmatrix} 1 & 0 & 0 & 0 & 0 & 0 & 0 \\ 0 & 1 & 0 & 0 & 0 & 0 & 0 \\ 0 & 0 & 1 & 0 & 0 & 0 & 0 \\ 0 & 0 & 0 & 0 & 1/\sqrt{2} & 0 & 1/\sqrt{2} \\ 0 & 0 & 0 & 0 & -1/\sqrt{2} & 0 & 1/\sqrt{2} \\ 0 & 0 & 0 & 1/\sqrt{2} & 0 & 1/\sqrt{2} & 0 \\ 0 & 0 & 0 & -1/\sqrt{2} & 0 & 1/\sqrt{2} & 0 \end{pmatrix} \tag{5.65}$$

2. Show that the new basis coordinates $\overline{x}^a$ and the new payoff fields $\overline{F}^j_{ab}$ are determined by the transformation S in exercise 1, where for the payoff fields we restrict the transformation to exclude the player inactive strategies:

$$\begin{aligned} \overline{x} &= S^{-1}x \\ \overline{F}^j &= S^{-1}F^j S \end{aligned} \tag{5.66}$$

3. Show that the transformation from the basis of Eq. (5.16) to that of Eq. (5.17) is accomplished through the transformation T below, with the transformations of the coordinates and payoffs being expressed analogously to Eq. (5.66):

$$T = \begin{pmatrix} 1 & 0 & 0 & 0 & 0 & 0 & 0 \\ 0 & 1 & 0 & 0 & 0 & 0 & 0 \\ 0 & 0 & 1 & 0 & 0 & 0 & 0 \\ 0 & 0 & 0 & 1 & 0 & 0 & 0 \\ 0 & 0 & 0 & 0 & 1 & 0 & 0 \\ 0 & 0 & 0 & 0 & 0 & 1/\sqrt{2} & -1/\sqrt{2} \\ 0 & 0 & 0 & 0 & 0 & 1/\sqrt{2} & 1/\sqrt{2} \end{pmatrix} \tag{5.67}$$

4. In this section, we have chosen the code of conduct based on the differences between the strategy to confess and the strategy to not confess. Rewrite the model and find the appropriate transformations if the code of conduct is to pick as inactive the strategy to confess for player 1 and the corresponding strategy for player 2.
5. Show that a model equivalent to the prisoner's dilemma is that of two players who have the choice to honor a contract or break the contract. This scenario is significantly more general than the prisoner's dilemma and underlies the ***invisible hand*** of (Smith, 1776).

6. For numerical work, the computations go faster if we have differential equations for $E^j{}_o$ and $E^j{}_\alpha$ even if these are given in terms of the inactive metric and E_{jo} and $E_{j\alpha}$ respectively. Show that the differential equations are:

$$\begin{aligned}
&\Delta_\upsilon E^j{}_o = q_\upsilon E^j{}_o + 2\theta_{\upsilon\alpha}E^{j\alpha} - f^j{}_{o\upsilon}\\
&\Delta_\upsilon E^j{}_\alpha = 2\omega_{\upsilon\alpha}E^j{}_o + \omega_{\upsilon\alpha}{}^\beta E^j{}_\beta - e_\alpha f^j{}_{o\upsilon}\\
&f^j{}_{o\upsilon} = 2\left(q_\upsilon E^{jo} + \left(\omega_{\upsilon\alpha} + \theta_{\upsilon\alpha}\right)\left(E^{j\alpha} + e^\alpha E^{jo}\right) + \omega_{\upsilon\alpha\beta}e^\alpha E^{j\beta}\right)\left(1 - E^k{}_o E_k{}^o\right)
\end{aligned} \tag{5.68}$$

7. Show that for the general case, the *bond compression* component Θ_υ, Eq. (5.48), satisfies the following equation:

$$\begin{aligned}
&\partial_\upsilon\Theta^\upsilon = \left(q_\upsilon + \Theta_\upsilon - \eta_\upsilon\right)\Theta^\upsilon - \kappa\left(\pi^\alpha{}_\alpha - n_i p + \frac{\mu - p}{n-1}n_i\right)\\
&\kappa p_{\alpha\beta} = \omega_{\alpha\upsilon'}{}^\upsilon\omega_{\beta\upsilon}{}^{\upsilon'} + 2\omega_{\upsilon\alpha}\omega^\upsilon{}_\beta - 2\theta_{\upsilon\alpha}\theta^\upsilon{}_\beta + \eta_\upsilon\omega^\upsilon{}_{\alpha\beta} + \kappa\pi_{\alpha\beta}
\end{aligned} \tag{5.69}$$

8. Show that for the general case, the *bond shear* components $\sigma_{\upsilon\alpha\beta}$, (5.48), satisfy the following equation:

$$\partial_\upsilon\sigma^\upsilon{}_{\alpha\beta} = \left(q_\upsilon + \Theta_\upsilon - \eta_\upsilon\right)\sigma^\upsilon{}_{\alpha\beta} - \kappa\left(\pi_{\alpha\beta} - {}^1\!/_{n_i}\, h_{\alpha\beta}\pi^\gamma{}_\gamma\right) \tag{5.70}$$

9. Show that for the streamline solutions of section 4.5, *the bond shear* and *bond compression* can be written in terms of potentials as follows:

$$\begin{aligned}
&\partial_\upsilon\omega_{\upsilon'\alpha\beta} - \partial_{\upsilon'}\omega_{\upsilon\alpha\beta} = 0\\
&\omega_{\upsilon\beta\gamma}\omega_{\upsilon'\alpha}{}^\gamma - \omega_{\upsilon\alpha\gamma}\omega_{\upsilon'\beta}{}^\gamma = 0\\
&\omega_{\upsilon\alpha\beta} = \partial_\upsilon\omega_{\alpha\beta}\\
&\Theta = h^{\alpha\beta}\omega_{\alpha\beta}\\
&\Theta_\upsilon = \partial_\upsilon\Theta\\
&\sigma_{\upsilon\alpha\beta} = \partial_\upsilon\sigma_{\alpha\beta} = \omega_{\upsilon\alpha\beta} - {}^1\!/_{n_i}\,\Theta h_{\alpha\beta}\\
&\partial_\upsilon\partial^\upsilon\sigma_{\alpha\beta} = \left(\partial_\upsilon q + \partial_\upsilon\Theta - \eta_\upsilon\right)\partial^\upsilon\sigma_{\alpha\beta} - \kappa\left(\pi_{\alpha\beta} - {}^1\!/_{n_i}\, h_{\alpha\beta}\pi^\gamma{}_\gamma\right)
\end{aligned} \tag{5.71}$$

10. Using the substitution defining the ***reduced bond shear potential*** $\bar\sigma_{\alpha\beta}$ in terms of the function Γ satisfying the first equation below, show that the equation for the *reduced bond shear* becomes as follows for the streamline solutions of section 4.5. In particular, this may hold when there is only a single active strategy or more generally, if all the compression matrices are proportional to each other:

$$\begin{aligned}
&\sigma^\upsilon{}_{\alpha\beta} = \Gamma^\upsilon\bar\sigma_{\alpha\beta}\\
&\partial_\upsilon\Gamma^\upsilon = \left(q_\upsilon + \Theta_\upsilon - \eta_\upsilon\right)\Gamma^\upsilon\\
&\partial_\upsilon\partial^\upsilon\sigma_{\alpha\beta} = \left(\partial_\upsilon q + \partial_\upsilon\Theta - \eta_\upsilon\right)\partial^\upsilon\sigma_{\alpha\beta} - \kappa\left(\pi_{\alpha\beta} - {}^1\!/_{n_i}\, h_{\alpha\beta}\pi^\gamma{}_\gamma\right)\\
&\Gamma^\upsilon\partial_\upsilon\bar\sigma_{\alpha\beta} = -\kappa\left(\pi_{\alpha\beta} - {}^1\!/_{n_i}\, h_{\alpha\beta}\pi^\gamma{}_\gamma\right)
\end{aligned} \tag{5.72}$$

11. The fastest signal between two points is along the null geodesic direction $g_{ab}dx^a dx^b = 0$. If equally spaced surfaces of constant *proper time* become compressed so that the corresponding intervals of time shrink, then show that the corresponding size of g_{tt} must grow to compensate. As a consequence, show that one expects that $g^{tt} \to 0$. The limit corresponds to the velocity along the null geodesic going to infinity. The ***causality principle*** is that this limit is not reached and $g^{tt} > 0$. For a single active dimension, show that the velocity along the null direction is:

$$c_{\pm} \equiv \left(\frac{du}{dt}\right)_{\pm} = \frac{g^{tu}}{g^{tt}} \pm \sqrt{\left(\frac{g^{tu}}{g^{tt}}\right)^2 - \frac{g^{uu}}{g^{tt}}} \tag{5.73}$$

12. Use Eq. (5.73) and the previous exercise to show that the requirement of a non-zero velocity along the null geodesic requires $g^{uu} < 0$. This is the ***principle of possible change*** that means any physical point must be able to move.
13. Show that for streamlines that have speeds close to unity in natural units, the causality principle narrows the size of the space: one gets a picture not unlike the physics picture of the big bang with a singularity at some finite point in the past in which space has zero size.
14. Show numerically that the speed along the null geodesics is ± 1 as seen in the proper distance—*proper time* plane. In the physical space, this corresponds to going along the diagonals of the contour mesh.
15. As an example of exercise 14, take the model of section 5.11 having high stakes and low beta and deduce that the vector direction δ^{μ}_{u} along du transformed to the co-moving frame is given by $E_{\mu}{}^{\alpha}\delta^{\mu}_{a} = E_{a}{}^{\alpha}$, Figure 5-44. There are clearly three areas where the magnitude of the vector vanishes, corresponding to where the streamlines bunch in Figure 5-43. Also show that the speed of null direction c_{+}, Eq. (5.73), is given by Figure 5-45. How do the corresponding speeds c_{-} behave? Show that the speeds can exceed unity, though they shouldn't become infinite.

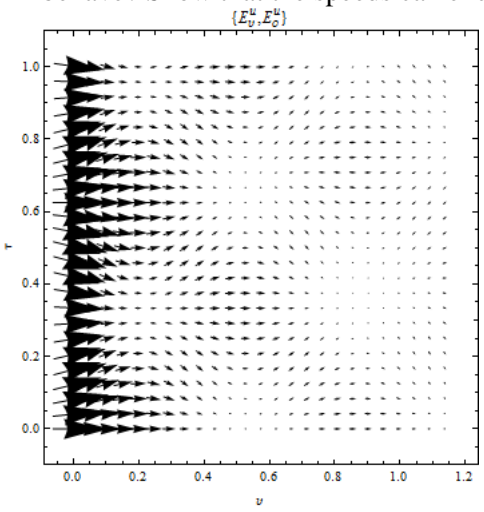

Figure 5-44: Vector field $\{E^{u}{}_{v} \quad E^{u}{}_{o}\}$ in the co-moving frame

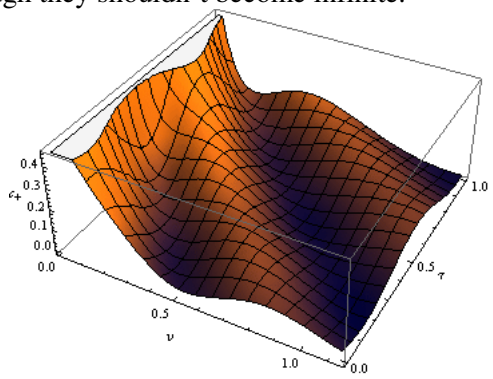

Figure 5-45: High stakes, low β, null direction speed c_{+}

16. Show that the active metric components Eq. (5.59) can be effectively written as the product of three matrices and so the determinant is given as stated below. Since for reasonable values of the variables, the determinant should not vanish or change sign, conclude that the coordinate vector along u can't vanish. What does this imply for exercise 15?

$$g^{ab} = \begin{pmatrix} E^{u}{}_{v} & E^{u}{}_{o} \\ E^{t}{}_{v} & E^{t}{}_{o} \end{pmatrix} \begin{pmatrix} -1 & 0 \\ 0 & 1 + e_{\alpha}e^{\alpha} \end{pmatrix} \begin{pmatrix} E^{u}{}_{v} & E^{u}{}_{o} \\ E^{t}{}_{v} & E^{t}{}_{o} \end{pmatrix}^{T} \tag{5.74}$$

$$\det g^{ab} = -\left(1 + e_{\alpha}e^{\alpha}\right)\left(E^{u}{}_{v}E^{t}{}_{o} - E^{t}{}_{v}E^{u}{}_{o}\right)^{2}$$

17. Show that another way to examine the behavior of high stakes and low β in exercise 15 is to look at the ***timeline*** and ***spaceline*** contours, Figure 5-46, associated with the time vector $\{E^{t}{}_{v} \quad E^{t}{}_{o}\}$, ("vertical" *timelines*) and the space vector $\{E^{u}{}_{v} \quad E^{u}{}_{o}\}$, ("horizontal" *spacelines*).

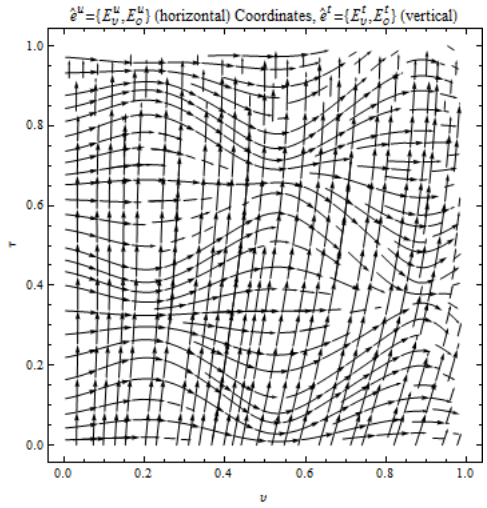

Figure 5-46: Coordinate timelines and spacelines for high stakes and low β

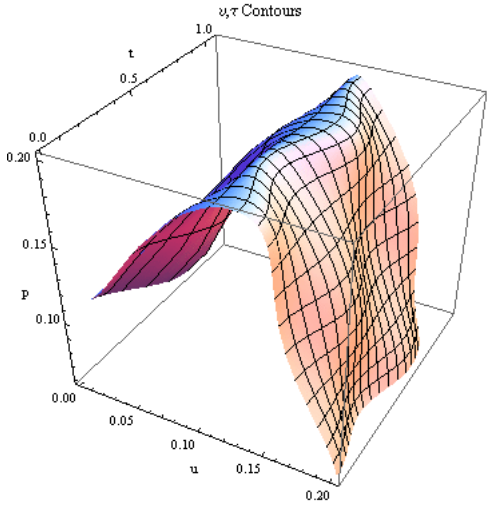

Figure 5-47: Pressure for high stakes and low β

18. For high stakes and low β in exercise 15, show that the pressure, which is a function only of v is not static, but has the shape given by Figure 5-47. Note that the pressure is in fact constant along each of the streamlines.
19. The *proper time* $\tau(u,t)$ and the proper distance $v = y^v(u,t)$ are each scalar functions. As an example, show that for high stakes and low β the scalar functions are given by Figure 5-48 and Figure 5-49, respectively.

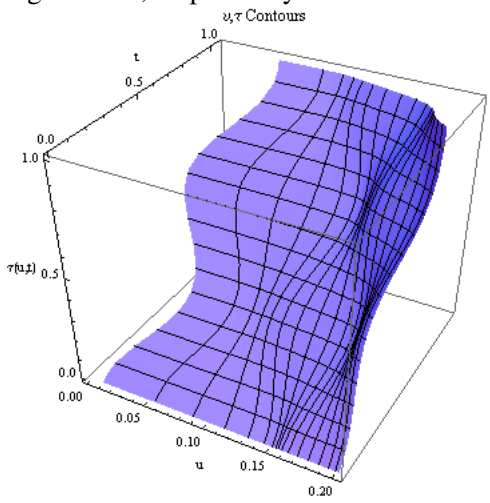

Figure 5-48: *Proper time* $\tau(u,t)$ for high stakes and low β

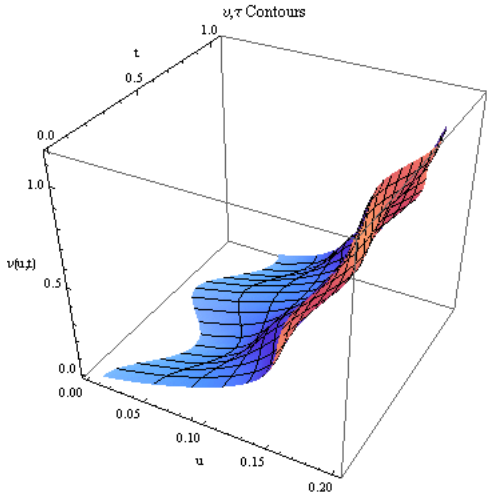

Figure 5-49: Proper distance $v(u,t)$ for high stakes and low β

20. For the examples given in the text, the flow $E^u{}_o$ along u need not be zero. Show that for high stakes and low β, the behavior remains *harmonic* as seen in the normal coordinate basis, Figure 5-50. For high stakes and high β show that the behavior is Figure 5-51.

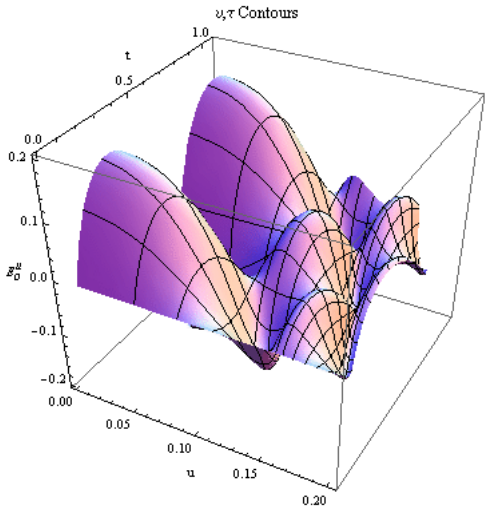

Figure 5-50: Flow along $E^u{}_o$ the focus direction for high stakes and low β

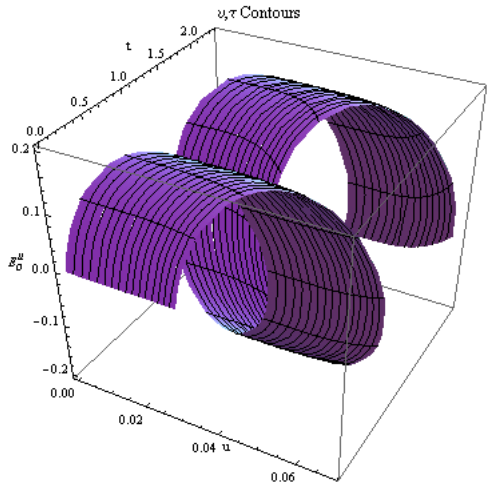

Figure 5-51: Flow along the focus $E^u{}_o$ direction for high stakes and high β

21. As seen in the previous exercise 21, for high stakes and high β, the scalar functions for *proper time* $\tau(u,t)$ and proper distance $\upsilon(u,t)$ take on strikingly new behaviors. Show that they are given by Figure 5-52 and Figure 5-53 respectively. What are the allowed regions? Argue that certain regions are excluded and indicate why.

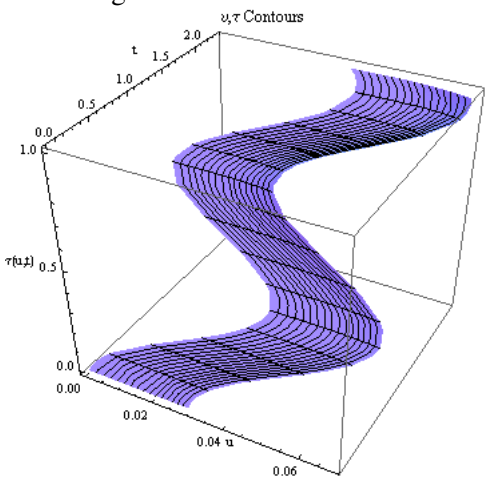

Figure 5-52: *Proper time* $\tau(u,t)$ for high stakes and high β

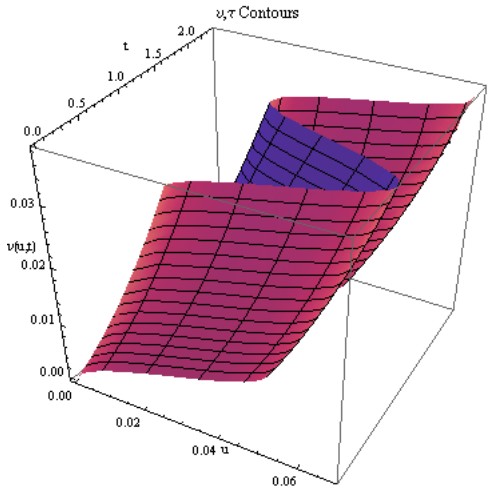

Figure 5-53: Proper distance $\upsilon(u,t)$ for high stakes and high β

22. *Proper time* as defined in section 4.5.2 is defined in terms of a specific path, the streamline. For the case of high stakes and small β, Figure 5-43, we can arrive at approximately the same point by two distinct streamlines from approximately the same start. In this case we expect that the proper times might be different since the coordinate $\mathbf{V} = \mathbf{E}^{\mathbf{o}}$ is not *exact* (section 4.2, Eq. (4.8)). Show that the figure shows evidence for this behavior. Pay particular attention to where the streamlines bunch together. Why is the flow not an *exact* differential?